REVIEW

Check for updates

Superparamagnetic iron oxide nanoparticles for magnetic hyperthermia: recent advancements, molecular effects, and future directions in the omics era

Carlotta Pucci, [iD] *[a] Andrea Degl'Innocenti,*[a,b] Melike Belenli Gümüş*[a,c] and Gianni Ciofani [iD] *[a]

Superparamagnetic iron oxide nanoparticles (SPIONs) have attracted attention in the biomedical field thanks to their ability to prompt hyperthermia in response to an alternated magnetic field. Hyperthermia is well known for inducing cell death, in particular in tumour cells, which seem to have a higher sensitivity to temperature increases. For this reason, hyperthermia has been recommended as a therapeutic tool against cancer. Despite the potentialities of this approach, little is still known about the effects provoked by magnetic hyperthermia at the molecular level, and about the particular cell death mechanisms that are activated. Nevertheless, in-depth knowledge of this aspect would allow improvement of therapeutic outcomes and favour clinical translation. Moreover, in the last few decades, a lot of effort has been put into finding an effective delivery strategy that could improve SPION biodistribution and localisation at the action site. The aim of this review is to provide a general outline of magnetic hyperthermia, focusing on iron oxide nanoparticles and their interactions with magnetic fields, as well as on new strategies to efficiently deliver them to the target site, and on recent *in vitro* and *in vivo* studies proposing possible cell death pathways activated by the treatment. We will also cover their current clinical status, and discuss the contributions of omics in understanding molecular interactions between iron oxide nanoparticles and the biological environment.

Introduction

Hyperthermia is a medical approach where the temperature of the body or of the target tissue is raised up to 40–45 °C. Since cancer cells seem to show a higher sensitivity to these temperatures with respect to healthy cells,[1–3] hyperthermia has been proposed as a non-invasive anticancer treatment, alone or in combination with chemo- and radiotherapy to improve their efficacy. Even though the mechanisms of hyperthermia-induced cell death in tumour cells have not been fully elucidated yet, its efficacy has been reported by several authors, and clinical trials involving hyperthermia started in the 1970s.[4] There are currently several methods to induce hyperthermia, such as exposure to microwaves, to electrode-applied high-frequency currents, and to lasers, or the immersion of the patient in heated water baths (whole-body hyperthermia).[5] However,

all these methods lack selectivity towards the target tissue, and might cause severe side effects on healthy cells. Therefore, more specific heating sources are preferable to enhance the therapeutic outcome. Magnetic hyperthermia opened new horizons in this sense; here, the rise in temperature is due to the heat produced by the interactions between magnetic nanoparticles and an appropriate alternated magnetic field (AMF). Magnetic hyperthermia offers several advantages with respect to conventional methods. First, magnetic nanoparticles can be functionalised on their surface with antibodies or ligands that can specifically target tumour cells, with very low accumulation in healthy tissues. Moreover, their heating capacity can be modulated by tuning their size, polydispersity, composition, and physicochemical properties, allowing for a better control of the desired outcome.[6] Magnetic nanoparticles can also act as magnetic resonance imaging (MRI) contrast agents;[7–9] therefore, they can be used for theranostic applications.[10,11] Among the different magnetic nanomaterials that can be used for this purpose, iron oxide-based nanoparticles, especially superparamagnetic iron oxide nanoparticles (SPIONs), seem to be the most promising, mainly because iron oxides have been approved by the US Food and Drug Administration,[12] and they are relatively easy to synthesise.[4] However, bare SPIONs are

[a]*Istituto Italiano di Tecnologia, Smart Bio-Interfaces, Viale Rinaldo Piaggio 34, 56025 Pontedera, Italy. E-mail: carlotta.pucci@iit.it, andrea.deglinnocenti@iit.it, melike.belenli@iit.it, gianni.ciofani@iit.it*

[b]*Università di Siena, Medical Genetics Unit, Viale Bracci 2, 53100 Siena, Italy*

[c]*Scuola Superiore Sant'Anna, The Biorobotics Institute, Viale Rinaldo Piaggio 34, 56025 Pontedera, Italy*

unstable in biological fluids; therefore, new solutions have been proposed to improve their solubility, bioavailability, and delivery to the target tissue.

Despite the massive effort that researchers have put into the study of SPION-induced magnetic hyperthermia, there is still little understanding of their mechanism of action at the molecular level. The lack of consensus is mainly due to the fact that magnetic hyperthermia can activate several cell death pathways, and the prevalence of one over the others depends on many parameters, such as the nanoparticles' properties, the frequency and intensity of the AMF, and cell typology, just to name a few.

The aim of this review is to provide an overview of magnetic hyperthermia induced by iron oxide magnetic nanoparticles (IONPs), and in particular by SPIONs, focusing on the physics behind their interaction with AMF. The latest strategies that demonstrate effective coating/functionalisation of the surface of SPIONs and their impact on SPION physicochemical properties, stability, biocompatibility, and bioavailability will be discussed, with some examples of efficient SPION-targeting ligand conjugates. An overview of the proposed mechanisms for the anticancer activity of SPION-induced magnetic hyperthermia will be provided, together with the most recent *in vitro* and *in vivo* studies focusing on this topic. Particular attention will also be paid to recent omics studies that can help to unveil mechanisms at the molecular level. Finally, a brief overview of clinical studies concerning SPIONs and magnetic hyperthermia will also be presented.

SPIONs and their interaction with AMFs

In nature, several types of iron oxides exist, differing in their chemical formula and/or crystalline structure.[13] Nevertheless, the most exploited for magnetic hyperthermia are magnetite and maghemite, thanks to their peculiar magnetic properties especially at the nanonascale.[6,14] The chemical composition of magnetite is $Fe^{2+}(Fe^{3+})_2(O^{2-})_4$ – hence, the chemical formula Fe_3O_4 – with a cubic inverse spinel structure, in which O^{2-} ions form a cubic structure and Fe^{2+} and Fe^{3+} occupy interstitial sites (1/3 tetrahedral and 2/3 octahedral sites).[15] The chemical formula of maghemite is Fe_2O_3, but it is often indicated as γ-Fe_2O_3 to differentiate it from hematite, another iron oxide with the same chemical formula, but different crystalline structure. Maghemite has the same spinel structure as magnetite, but only Fe^{3+} is present; for this reason, maghemite is considered a fully oxidised magnetite.[15] Both magnetite and maghemite are ferrimagnetic, meaning that they are composed of two populations of atoms with antiparallel magnetic moments – like in antiferromagnetism – but one of the two populations prevails; therefore, the materials possess a net magnetic moment different from zero.[16] When an external magnetic field is applied, all the magnetic moments align with its direction until a magnetisation saturation (M_S) is reached. When the magnetic field is removed, the magnetisation does not spontaneously revert completely to the initial value, but there will be a remanent magnetisation (M_R), and a precise magnetic field, called the coercivity field (H_C), must be applied to bring the system to the initial state.[4,16] Under AMFs the magnetic moment direction cannot change instantaneously with the AMF and a delay in the magnetic response is produced, causing a hysteresis loop in the magnetisation cycle (Fig. 1a).[4,16]

Bulk iron oxide is a multi-domain magnet, constituted by several magnetic domains; in this case, the origin of the hysteresis is due to reorganisation or to domain wall motions.[16] The energy dissipated in the magnetisation cycle (hysteresis losses) produces heat, and its entity can be calculated from the area of the hysteresis loop (Fig. 1a).[4]

IONPs below a critical diameter ($\approx$30 nm[6,14]) behave as single-domain magnets with superparamagnetic properties.

Carlotta Pucci

Carlotta Pucci was awarded her PhD in Chemical Sciences at the University of Rome "La Sapienza" (Italy) working on the synthesis of liposomes and on the study of their interactions with biomacromolecules. She is currently a postdoctoral fellow in the Smart Bio-Interfaces Research Line of the Italian Institute of Technology (IIT) in Pontedera, Italy. She specializes in the fabrication and characterization of different kinds of biocompatible and multifunctional nanomaterials for the treatment of central nervous system diseases.

Andrea Degl'Innocenti

Andrea Degl'Innocenti is a researcher at the University of Siena (Unisi) and the Italian Institute of Technology (IIT). His alma mater is the University of Pisa, Italy; there he obtained his BSc and MSc (with honors) in molecular biology. He then pursued his doctoral studies in Germany, working on the genetics of smell at the Max Planck Institute for Brain Research. After spendin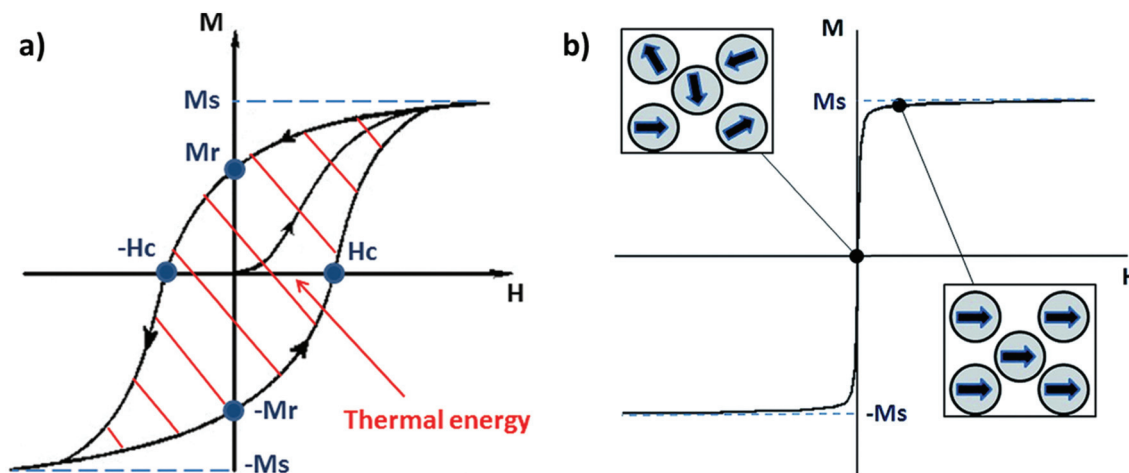g some more time at the institute as a postdoc he joined IIT, and finally Unisi. Currently, he studies human genomics in COVID-19, as well as space-elicited oxidative imbalance with omic approaches. Other interests include neurobiology and senses.

Fig. 1 (a) Typical hysteresis loop of a ferrimagnet. M_s and M_r are, respectively, the magnetisation saturation and the remanent magnetisation, while H_c is the coercivity field. The area depicted by the red lines is the energy dissipated during a magnetisation cycle. (b) Typical magnetisation cycle for a superparamagnetic material (above the blocking temperature); the squares depict the orientation of the moment of single-domain nanoparticles with the external magnetic field (H). Reproduced and adapted with permission from ref. 4. Copyright RSC, 2014.

SPIONs have zero coercivity and zero remanent magnetisation; however, they have large magnetic susceptibility – the extent to which a material can be magnetised upon application of an external magnetic field – with respect to paramagnets. When SPIONs are subjected to an AMF, the magnetic moments of the single nanoparticles (magnetic domain) align with the direction of the applied field reaching $+M_S$ (or $-M_S$) depending on the direction; however, since SPIONs have no remanent magnetisation and coercivity, their magnetisation curve significantly differs from that observed in bulk iron oxide (Fig. 1b). Moreover, in SPIONs, the mechanisms of heat generation due to relaxation losses also differ from those that prevail in multi-domain iron oxides. During a magnetisation cycle of SPIONs, there are essentially two ways to relax back to the initial state when the field is removed: Néel and Brownian relaxations.[4] In Néel relaxation, the magnetisation of the single nanoparticle can rapidly flip direction with a characteristic time defined as the Néel relaxation time, τ_N, that depends, among other parameters, on the particle size and magnetic anisotropy, and on the temperature of the medium, as expressed by the equation:

$$\tau_N = \tau_0 \exp\left(\frac{KV}{k_B T}\right) \tag{1}$$

where τ_0 is a characteristic of the material, named the attempt time or attempt period (usually between 10^{-10} and 10^{-9} s), K is the anisotropy constant, V is the volume of the nanoparticle, k_B is the Boltzmann constant, and T is the temperature. Usually, at temperatures higher than the blocking temperature T_B, that is the temperature below which the magnetic moments do not have the required energy to flip directions

Melike Belenli Gümüş is a third-year PhD student in the joint program between The Biorobotics Institute of Sant'Anna School of Advanced Studies and the Italian Institute of Technology (IIT). She conducts her research activities under the supervision of Prof. Gianni Ciofani in the Smart-Bio Interfaces Research Line at the IIT. Her research interests include smart nanomaterials for targeted drug delivery and Raman spectroscopy applications at the nano–bio interface.

Melike Belenli Gümüş

Gianni Ciofani, PhD, is Research Director at the Italian Institute of Technology, where he is Principal Investigator of the Smart Bio-Interfaces Research Line and Coordinator of the Center for Materials Interfaces (Pontedera, Italy). His main research interests are in the field of smart nanomaterials for nanomedicine, bio/non-bio interactions, and biology in altered gravity conditions. He is coordinator or unit leader of many grants/projects, and in 2016 he was awarded a European Research Council (ERC) Starting Grant.

Gianni Ciofani

(for instance, T_B is reported to be <100 K, for oleic-acid stabilised SPIONs of ≈10 nm, when no external magnetic field is applied[17]), and given the measuring times of conventional techniques, the net magnetisation of SPIONs is, on average, equal to zero. As is evident from eqn (1), the smaller the nanoparticles, the lower the energy necessary to flip the magnetic moment. In Brownian relaxation, the nanoparticle and its magnetic moment rotate together, causing frictions with the liquid where the particle is dispersed. The Brownian relaxation time, τ_B, is defined by the equation:

$$\tau_B = \frac{3\eta V_H}{k_B T} \qquad (2)$$

where η is the viscosity of the medium and V_H is the hydrodynamic volume of the nanoparticles. For this relaxation mechanism, the viscosity of the medium plays a fundamental role. Brownian relaxation, in fact, is almost negligible for small particles in high-viscosity media, where Néel relaxation prevails.[4] The prevalence of one mechanism over the other mainly depends on the size of the particles, on their magnetic anisotropy, and on the viscosity of the liquid.

Under an appropriate high-frequency AMF, that is, when the magnetic field direction changes faster than the relaxation time of the nanoparticles, the reversal of the magnetic moments is delayed, causing losses and consequently heat dissipation.

The heat power generated by magnetic nanoparticles upon AMF stimulation can be quantified by adapting the general concept of specific absorption rate, or SAR, (in W g^{-1}) to this specific case:

$$SAR = C \frac{\Delta T}{\Delta t} \frac{1}{C_{Fe}} \qquad (3)$$

where C is the specific heat capacity of the sample, $\Delta T/\Delta t$ is the initial slope of the time-dependent heating curve, and C_{Fe} is the iron concentration. The SAR of magnetic nanoparticles depends not only on their properties such as size, polydispersity, and saturation magnetisation, but also on the frequency and amplitude of the AMF; in particular, the higher these two values, the higher the SAR. However, for biomedical applications the product between the intensity and the frequency of the magnetic field ($H \times f$) should be lower than 5×10^8 A m^{-1} s^{-1} to avoid negative effects on patients.[5] In fact, Atkinson et al. observed that, when $H \times f$ is above this limit (known as the "Brezovich limit"), the occurrence of eddy currents might generate an unpleasant non-specific heating.[18] Superparamagnetic materials such as SPIONs are, generally, preferred for biomedical applications with respect to ferrimagnetic bulk materials. First of all, superparamagnetism is achieved at the nanoscale; moreover, SPIONs generate heat through Néel and Brownian relaxations – superimposed on ferrimagnetic hysteresis losses at the transition between superparamagnetism and ferrimagnetism – that result in higher SAR values at lower fields and frequencies with respect to the hysteresis losses in ferrimagnetic bulk iron oxides.[16] This means that higher effects can be achieved at lower $H \times f$.

Finally, SPIONs have zero net magnetisation, meaning that they do not aggregate.[4] However, their incompatibility with aqueous environments makes their dispersion in biological fluids quite challenging. Moreover, it must be stressed that, for biological applications, nanoparticles relaxing via Néel mechanisms are preferable, since the intracellular viscosity might prevent Brownian relaxation.[19]

Magnetic hyperthermia is usually achieved by stimulating SPIONs with AMF, the frequencies of which range from 100 to 800 kHz. Nevertheless, even if beyond the scope of this review, it is worth mentioning that a biological effect could be observed also at very low frequencies (<1 kHz), defined as non-heating low frequencies, and it is ascribed to mechanical effects on the surrounding tissues caused by the vibrations and rotations of magnetic nanoparticles under an external magnetic field.[20,21]

Recent delivery and targeting technologies for SPIONs

Many applications benefit from the physicochemical properties of SPIONs. A remarkable number of these applications concentrate on the use of SPIONs for diagnostic and theranostic purposes. Their superparamagnetic properties make them advantageous for MRI,[22] magnetic hyperthermia,[23] and targeted drug delivery.[24] The incorporation of SPIONs into a drug carrier[25] and/or modifications on their surfaces[26] enable them to be targeted to many different tumour tissues such as prostate cancer,[25] breast cancer,[26] bone cancer, and brain cancer.[27] The major drawback of using SPIONs in biological applications is their instability and tendency to form aggregates through van der Waals interactions in aqueous environments, which results in their incompatibility with physiological fluids.[28] Aggregation/agglomeration of SPIONs may favour magnetic dipolar interactions between particles, and these interactions can affect their intrinsic magnetic properties depending on the aggregation state of SPIONs.[29] Moreover, the formation of bigger aggregates may increase the risk of recognition by the reticuloendothelial system (RES).[22] Therefore, many studies have been focused on increasing the bioavailability and biodistribution of SPIONs by proper surface modifications, which enhance their biocompatibility and stability in physiological fluids without losing their magnetic properties. Coating the surface of SPIONs with a biocompatible polymer is one of the most common ways to achieve this purpose. Besides increasing SPION stability and water solubility, polymers can also be modified with functional groups to have moieties on the surface that may allow further functionalisation with antibodies,[30] peptides,[31] or vitamins,[32] for instance. In addition to polymers, the surface of SPIONs can be coated with small molecules,[33] lipids,[34] and carbon/silica composites[27] to increase their colloidal stability in physiological fluids and provide an active surface for targeting ligands, with minimal effects on their magnetic properties. In this section, the latest delivery methods to increase the bio-

availability of SPIONs along with targeting strategies that are necessary for imaging and cancer therapy applications will be discussed.

Stabilisation in aqueous environments and bioavailability

The usual synthetic routes for SPIONs vary from physical to chemical methods. Nevertheless, there are also a few studies showing that they can be biosynthesised by magnetotactic bacteria[35] and, *in situ*, by cancer cells.[36] Thermal decomposition is one of the most popular chemical synthesis methods for SPIONs, in the presence of oleic acid as the surfactant. SPIONs with oleate groups on their surface have good dispersibility in apolar (organic) solvents, but to use them in *in vitro* or *in vivo* experiments, they should be well dispersed also in polar solvents. This can be obtained by using amphiphilic molecules to cover the surface of SPIONs; the hydrophobic part of the molecule interacts with the surface of SPIONs, while the hydrophilic residues are exposed to water molecules, giving the nanoparticle aqueous stability.[37]

Biocompatible polymers are mostly preferred to stabilise SPIONs in water. For example, Galli *et al.* modified polyamidoamine (PAA) by reacting 17% of the carboxyl groups of PAA with the amine group of 2-nitrodopamine. Catechol groups, which have high affinity with iron, are present in the 2-nitrodopamine structure. A low amount of catechol functionalisation did not cause any disturbance of PAA structure, while providing colloidal stability to nanoparticles.[37] Polyethylene glycol (PEG) is one of the most versatile polymers that has been widely used in industrial and commercial products, as well as pharmaceutical ones. PEG, alone or as a copolymer, is also widely used in the synthesis of different kinds of nanomaterials as it provides surface stabilisation by increasing steric hindrance, and it protects the nanoparticles from adsorption of macromolecules.[38]

Yan and co-workers investigated the biodistribution of SPIONs in rat brains by coating their surface with PEG. The presence of PEG on the surface increased the hydrophilicity of particles, and provided a slightly negative zeta potential on the surface. PEG-SPIONs were injected into the substantia nigra area in the midbrain of rats and the particles were found also in nearby structures such as the thalamus, temporal lobe, olfactory bulb, and prefrontal cortex. The subcellular distribution of PEG-SPIONs in the substantia nigra area revealed that they are mainly concentrated near dendrite and axon membranes.[39] In another work, SPIONs were coated with poly (lactic-*co*-glycolic acid) (PLGA) by using different surfactants. Two types of PLGA-coated SPIONs with differences in sizes and surface charges were obtained, as the surfactants used in the preparation method had different chemical properties: the strong cationic nature of didodecyl-dimethylammonium-bromide resulted in nanoparticles (DMAB-SPIONs) with higher positive zeta potential (+54 mV) and smaller average hydrodynamic diameter (30 nm) with respect to particles coated with α-tocopheryl-polyethylene-glycol-succinate (TPGS-SPIONs), 180 nm in size and with a zeta potential of +35 mV. Both particles were orally introduced to adult male Swiss albino mice

and their accumulation in different organs was evaluated. In the brain tissue of DMAB-SPION treated mice, a significant amount of iron was detected, proving that DMAB-SPIONs diffused through the blood–brain barrier (BBB). On the other hand, TPGS-SPIONs were mostly observed in Kuppfer cells of the liver, which are associated with phagocytic activity. In addition to that, liver function enzyme levels were increased in mice treated with TPGS-SPIONs, indicating a certain amount of damage due to the presence of the nanoparticles.[40] In another recent study, polyaniline and polypyrrole were separately used to modify the surface of SPIONs. From the preliminary hyperthermia and cytotoxicity results, it was shown that coated SPIONs have slightly higher saturation magnetisation values and both coatings have a positive effect on the biocompatibility of the SPIONs.[41]

Core–shell nanocomposite materials are another "hot topic" for introducing SPIONs to biological fluids. Inorganic compounds such as calcium phosphate,[42] metallic materials such as silver (Ag) and gold (Au),[43] and biocompatible polymers such as PEG can be used in composite structures.[44] Covering the surface of SPIONs with silicon dioxide (SiO_2), which is a widely used material for ceramic coating, is another route to obtaining controllable surface chemistry on SPIONs. Silica coating increases the colloidal stability, reduces toxicity, and protects the magnetic cores from oxidation. Moreover, silanol groups of silica enable surface functionalisation of the nanocomposites.

Santos *et al.* prepared a theranostic nanoplatform that takes advantage of the interaction between Fe^{3+} ions and curcuminoids (fluorescent biomarkers) based on iron–oxygen coordination and hydrogen bonding. Then, curcuminoid-adsorbed SPIONs were further coated with silica to have good colloidal stability and dispersibility in water. This nanoplatform showed promising results in terms of magnetic hyperthermia and fluorescent imaging, but further *in vitro* and *in vivo* studies are necessary.[45] Another interesting example of a stabilisation and delivery strategy for SPIONs is represented by "earthicles", which are nanocomposites consisting of zero-valent iron, silica, and carbon, with a composition that resembles the stratified structure of the Earth (and thus the reason for their name). Wu *et al.* prepared earthicles with a ferrofluid core containing SPIONs instead of a zero-valent iron core; the coating, composed of a double shell of silicate mesolayers (SiO_2) and carbon (C) crust, was kept similar to the original earthicles' composition. The coating provided stability by means of electrostatic effects and allowed ligand conjugation to the surface for targeting purposes. These particles were tested against glioblastoma and osteosarcoma cells/spheroids and gave promising results for the treatment of these challenging types of cancer. $SPION/SiO_2/C$ colloids show higher specific saturation magnetisation as a result of the hydrothermal processing during their synthesis. Thanks to the ferrofluid nature of the core, they can be guided to the tumour area by a conventional magnet. According to BBB permeability experiments on both *in vitro* and *in vivo* models, the SiO_2/C shell protects the particles against lysosomal degradation and enables transcel-

lular passage of SPIONs.[27] Calcium phosphates and their naturally occurring form, hydroxyapatite, have been also combined with SPIONS to form composite materials; in particular, they have been exploited to coat the surface of SPIONs, increasing their biocompatibility, and providing pH-responsive properties to the composite nanoparticles that can be beneficial in cancer therapy.[42,46] Another strategy that helps in stabilizing the surface of SPIONS is coating them with metals, such as Ag and Au. This also enables use of the composites in photothermal therapy, and facilitates the functionalisation of the nanocomposite surface for targeted cancer therapy applications.[43,47] As an example, Lu *et al.* targeted human glioma cells by using core–shell Fe_3O_4@Au magnetoplasmonic nanomaterials functionalised with the antibody cetuximab (C225). The coating with Au provides a biocompatible layer, enables a stable interaction with the antibody, and allows for local plasmonic heating upon stimulation with a near-infrared (NIR) laser. *In vitro* studies with glioma cells and *in vivo* studies with animal models revealed the synergic effect of the magneto-photothermal strategy by showing increased apoptosis and decreased tumour size with respect to the separate treatments with just AMF or NIR.[48]

Covering the outer surface of nanoparticles with biological macromolecules is another well-known strategy to increase their stability, biocompatibility, and circulation time in the body by shielding them from being recognised by the RES. Lipid nanocarriers are among the best candidates for drug delivery applications, and many lipid-based formulations are already available for clinical use.[49] Lipid vesicles loaded with SPIONs are known as magnetoliposomes,[50] and depending on the application these lipid carriers can have a third component such as an inorganic silica shell.[34] Magnetoliposomes have many advantages: their lipid surface mimics natural cell membranes and decreases the rate of clearance by the RES, the functionality of the lipids can be easily modified, different types of drugs (hydrophobic, hydrophilic and amphiphilic) can be encapsulated inside or in the lipid bilayer, and their temperature-dependent permeability allows for controlled drug release, thanks to the heat generated by the SPIONs upon AMF stimulation.[50] In addition, Patil-Sen and co-workers reported that a coating made both of lipids and silica decreased the T_2 relaxation time of SPIONs, enhancing the quality of MRI imaging.[34]

Another class of macromolecules that can be used for the stabilisation of SPIONS is carbohydrates.[28] Some of the most widely used polysaccharides for coating the surface of SPIONS are dextran and its derivatives. Although dextran-coated IONPs are already commercially available, this type of coating can also bring some disadvantages such as quick degradation of dextran by enzymes in the human body, causing loss of stabilisation. To overcome this problem, inulin, a plant-derived polysaccharide, was proposed for the stabilisation of the SPION surface. This polysaccharide cannot be digested by enzymes in the human body, while maintaining the advantages of other carbohydrates.[22] Some studies, instead, proposed the synthesis of iron oxide nanoparticles with a green approach, where

Garcinia mangostana fruit peel extracts were used, which are rich in polyphenols that can act as stabilisers.[51]

Dimercaptosuccinic acid (DMSA) is a metal chelator used for the treatment of heavy metal poisoning. It is a water-soluble and non-toxic molecule that can be grafted on the surface of oleate-stabilised SPIONs by ligand exchange reaction. It provides a stable surface even in acidic conditions thanks to its negatively charged carboxylate ions on the outer surface; these carboxyl groups, together with thiol groups, enable further functionalisation. For example, after the modification of the SPION surface with DMSA, peptide nucleic acids (PNA) can be attached to the surface by Michael addition. These hybrid nanomaterials can be useful for targeting non-coding microRNAs, which are responsible for certain inflammatory and autoimmune diseases.[33] Table 1 summarises all the types of SPION coating that have been cited in this review.

Targeting

In order to maximise the concentration of SPIONs in the diseased area and minimise negative side effects on healthy cells, an efficient targeting strategy is necessary. There are three main routes for the delivery of SPIONs in the desired site: passive targeting, delivery with an external magnet, and active targeting. The passive targeting strategy exploits the enhanced permeability and retention (EPR) effect that derives from the increased vascular permeability of abnormally formed tumour mass and from the deficiency of the lymphatic system around the tumour, phenomena that cause the retention of particles in that area.[28,66] Thanks to their magnetic properties, the delivery of SPIONs can also be externally manipulated by applying an external magnetic field to guide them towards the area of interest.[27] The last and generally preferred method for SPIONs' delivery is the so-called "active targeting", that exploits the functionalisation of the SPION surface with suitable molecules (ligands) that interact with specific receptors overexpressed by the target cells.[66]

Briefly, the main idea is first to achieve SPIONs with colloidal stability in physiological fluids by coating them with biocompatible stabilisers that are also eligible for further functionalisation. Then, the ligand can be attached to the surface *via* strong electrostatic interactions or with an appropriate chemical reaction between the surface functional groups and a chemically active moiety of the targeting molecule.[23] Peptides are widely used for targeting purposes in various drug delivery systems. There are many examples of SPION–peptide conjugates that are designed to deliver SPIONs effectively to the targeted cells/tissue/organs, for both diagnostic and therapeutic applications. As an example of MRI application, a high-affinity peptide (aptide) ligand (APT_{EDB}) for targeting extra domain-B fibronectin (EDB-FN), which is a hypothesised biomarker for breast tumour initiating cells (BTICs), was conjugated to SPIONs. In Fig. 2, the histological analysis of tumour tissues taken from mice injected with APT_{EDB}-conjugated SPIONs and $APT_{scramble}$-conjugated SPIONs (as control group) revealed that the APT_{EDB}-conjugated SPIONs were distributed at a higher extent in the areas where EDB-FN expression was high. In con-

Table 1 Examples of SPION coating cited in this review. Names of the coating components, their typology, and the reference where they have been used are listed

Coating	Material type	Ref.
Glyceryl monooleate (GMO)	Lipid	52
N-Palmityl-6-nitrodopamide (P-NDA)	Lipid	50
Silica/lipid (dipalmitoyl phosphatidylcholine (DPPC)/cholesterol (Ch) mixture)	Inorganic inner shell–lipidic outer shell	34
Silica (SiO_2)	Inorganic	45
Silica/carbon (earthicles)	Inorganic double shell	27
Inulin-based silica	Inorganic inner shell–polysaccharide outer shell	22
Calcium phosphate ($Ca_3(PO_4)_2$)	Inorganic	42 and 53
Hydroxyapatite (HAP)	Inorganic	46
Silver (Ag) and gold (Au)	Metallic shell	43, 47 and 48
Hyaluronic acid (HA)	Polysaccharide	26
β-Cyclodextrin (β-CD)	Oligosaccharide	28
Dimercaptosuccinic acid (DMSA)	Small molecule	33 and 54
Plant extract	Mixture of small organic molecules	55
Poly(lactic-co-glycolic acid)–poly(ethylene glycol) di-block copolymer (PLGA-b-PEG)	Polymer	56
Polyethylene glycol (PEG)	Polymer	39 and 57–60
Poly(acrylic acid) (PAA)	Polymer	61
Poly(D,L-lactide-co-glycolide) (PLGA)	Polymer	31 and 40
Polyaspartamide (PA)	Polymer	32
Polyaniline	Polymer	62
Polypyrrole	Polymer	62
Poly-D-lysine/polyethylene glycol/pH low insertion peptide (PDL–PEG$_{24}$–pHLIP)	Polymer	63
Pluronic F127	Poloxomer (polymer)	64
Polyamidoamine (PAA)	Dendrimer (polymer)	65

trast, a lower amount of SPIONs was detected in APT$_{scramble}$-conjugated SPION-injected mouse tumours. This proved the specificity of APT$_{EDB}$ peptide to EDB-FN; hence, their conjugation to contrast agents like SPIONs makes visualisation of BTICs in the tumour tissue possible.[59] A similar but more recent study showed the possibility of using MRI and magnetic particle imaging (MPI) for image-guided hyperthermia studies. The surface of IONPs was modified with the peptide CREKA, a ligand for fibrin–fibronectin complexes, to obtain a more homogeneous distribution of IONPs throughout the tumour area. The proposed combination of multimodality imaging and the targeting agent has been tested on a tumour-bearing mouse model, and a successful targeting and a significant decrease in tumour size were observed after stimulation with the AMF.[60] In an interesting study by Wei et al., the acidic microenvironment of tumour tissue was exploited to target SPIONs as contrast agents. They formulated SPION nanoclusters by using poly-D-lysine (PDL); this synthetic polymer was PEGylated and a pH (low) insertion peptide (pHILP) was conjugated to it through the PEG linker molecule. Conformational changes of pHILP due to the lower pH values of the tumour microenvironment facilitated the accumulation of SPIONs into tumour cells; hence, a tumour-selective imaging could be achieved.[67]

The surface of SPIONs can be modified with other cell-specific molecules such as antibodies,[30] vitamins,[68] monosacharides,[69] and small molecules[70] in a similar fashion. Some cell-based approaches have also been developed for the delivery of SPIONs. Singh and co-workers used mesenchymal stem cells (MSCs) as delivery vehicles for magnetic nanoparticles that are codelivered with a drug molecule. They observed the inhibition of tumour growth as a result of magnetic hyperthermia combined with chemotherapy.[52]

Overall, thanks to various surface modifications and further functionalisation of SPIONs, it is possible to use their unique magnetic properties in in vitro and in vivo applications that require multidimensional approaches. The most important results of these developing technologies are that they may enable early detection of cancer and monitoring of the treatment by non-invasive methods, while providing a combinatory therapy of hyperthermia and targeted drug delivery.[25]

Cell death mechanisms induced by SPIONs and magnetic hyperthermia: recent in vitro and in vivo studies

The biological mechanisms behind the toxicity of magnetic hyperthermia have not yet been fully elucidated. The main reason for the lack of consensus is that the effects of magnetic hyperthermia depend on several factors, including the physico-chemical properties of the nanoparticles used, their concentration, their intracellular location, and the cell type, for instance.

Beola et al. demonstrated that, depending on the concentration of the SPIONs, the AMF stimulation might trigger extrinsic (e.g., caspase-8-mediated apoptosis) or intrinsic (e.g., increased Bax/bcl-2 ratio) death pathways.[71] In particular, they showed that at the lowest SPION concentrations tested, the
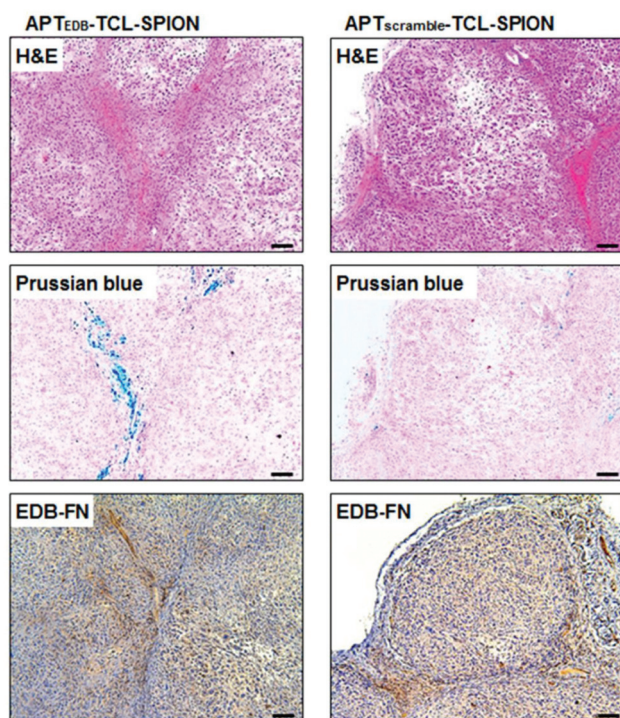
Fig. 2 Histological analysis of tumour tissues from breast tumour-bearing mice. Hematoxylin and eosin (H&E) staining to investigate histological changes, Prussian blue staining to detect SPIONs, and EDB-FN immunostaining to evaluate EDB-FN expression levels were performed. The blue dots in Prussian blue staining show the SPIONs in the tumour tissues obtained from mice injected with APT_{EDB}-conjugated SPIONs and $APT_{scramble}$-conjugated SPIONs. Accumulation of APT_{EDB}-conjugated SPIONs with respect to $APT_{scramble}$-conjugated SPIONs can be clearly seen. Reproduced with permission from ref. 59. Copyright Ivyspring International Publisher, 2014.

AMF stimulus triggered a decrease of B-cell lymphoma 2 (Bcl-2) mRNA expression and a contextual overexpression of the Bcl-2 associated X protein (Bax) mRNA levels, with consequent increase of the Bax/Bcl-2 ratio. Bax (pro-apoptotic) and Bcl-2 (anti-apoptotic) proteins are linked to the intrinsic cell death pathway *via* mitochondria permeabilisation. On the other hand, upon AMF stimulation, the highest SPION concentrations tested induced caspase-8 activation without an increase of the Bax/Bcl-2 ratio, suggesting mainly an extrinsic death pathway. Therefore, by just varying the intracellular nanoparticles' concentration, one particular cell death pathway can be more evident than others. Nevertheless, both intrinsic and extrinsic pathways can be activated by several mechanisms. For instance, intrinsic pathways are activated when a stress such as oncogene activation (*e.g.*, TP53), DNA damage, hypoxia, or survival factor deprivation occurs within the cell. Extrinsic pathways, instead, are activated when the cytotoxic stress is induced in the extracellular environment or when "death receptors" expressed on the cell surface are activated by specific "death ligands". Typical death receptors are CD95 (APO-1/Fas), TNF receptor 1 (TNFRI), TNF-related apoptosis-inducing ligand-receptor 1 (TRAIL-R1), and TRAIL-R2,

and their corresponding ligands are the CD95 ligand (CD95L), TNFα, lymphotoxin-α, and TRAIL.[72] Adamiano *et al.* studied the effects of magnetic hyperthermia induced by two types of superparamagnetic nanomaterials: iron-doped hydroxyapatite (FeHA) and IONPs coated with amorphous calcium phosphate (Mag@CaP).[53] The authors demonstrated that, regardless of the type of nanoparticles, their efficient internalisation was crucial in eliciting a significant reduction of cancer cell viability. Nevertheless, even though FeHA were better internalised by the cells, Mag@CaP were more effective in inducing apoptosis; this might be linked to different physicochemical properties, particle–particle interactions, and different AMF absorption rate. Therefore, the physicochemical features of the nanoparticles may have an impact not only on the efficacy of the treatment, but also on its mechanisms of action.

In the past few years, researchers have devoted a fair amount of work to understanding the mechanisms of cell death activated by stimulation of SPIONs with AMF. Many studies suggested that several pathways can be involved at the same time. One of the most straightforward explanations for SPION-mediated magnetic hyperthermia toxicity was, simply, a direct consequence of the increased overall intracellular temperature upon AMF stimulation. Hyperthermia has been shown to induce proteins' unfolding and aggregation, and, when nuclear proteins are involved, an impairment of the DNA replication forks and DNA damage, such as a double strand break, can be observed.[73] However, unfolding of proteins at temperatures induced by hyperthermia (40–45 °C) is often efficiently counteracted by the expression of molecular chaperones, such as the "heat shock proteins" (HSP), and in particular by the HSP 70.[73] Hyperthermia can also affect plasma membrane permeability; this causes a calcium spike with consequent alterations of the mitochondrial membrane potential and change in the redox state of the cell.[73] An increase of plasma membrane permeability in glioblastoma multiforme cells exposed to magnetic hyperthermia triggered by SPIONs + AMF was, indeed, observed by Marino *et al.*[74]

All these mechanisms, however, can also be triggered in healthy cells; therefore, they do not entirely describe the higher sensitivity of cancer cells to magnetic hyperthermia.[1] Moreover, while diffused thermal effects might be a good explanation when high intracellular concentration of SPIONs and/or high $H \times f$ are used,[75,76] they do not account for the induced toxicity in systems with low or no measurable increase of temperature. As a matter of fact, as already said in the previous sections, due to the high viscosity of the intracellular environment, Brownian relaxations are mostly quenched and Néel relaxation mechanisms prevail; therefore, depending on the nanoparticles, the heat transfer could be very low or even negligible. Moreover, it has been demonstrated that, even if a global increase in temperature in the sample cannot be detected, the temperature in the close vicinity of a magnetic nanoparticle upon AMF stimulation might be very high, and it quickly decays with distance. For example, Riedinger *et al.* were able to measure *in vitro*, with a subnanometer resolution, the temperature profile at the nanoparticle surface, thanks to a

fluorescent probe (fluoresceinamine) conjugated to IONPs functionalised with PEG of different molecular weights through a thermo-sensitive linker (azobis[*N*-(2-carboxyethyl)-2-methylpropionamidine]).[77] The authors reported a high local heating, with temperatures reaching 45 °C at distances <0.5 nm from the nanoparticle surface (AMF parameters: 334.5 kHz, 17 mT); however, the temperature was found to exponentially decay with distance. More recently, Silva *et al.* were able to map the intracellular increase in temperature as a response to magnetic hyperthermia in green fluorescent protein (GFP)-expressing cancer cells (HeLa cells) *in vitro*.[78] The authors were able to correlate the fluorescence lifetime of the GFP to the local temperature, and showed that cells treated with 50 μg mL^{-1} polyacrylic acid-coated IONPs (<20 nm) and stimulated with AMF (499 kHz, 20 mT) experienced a heterogeneous temperature increase (±30 °C) in different areas of the cell. In particular, the highest temperatures (>70 °C) were reached in the areas where the nanoparticles were concentrated. These works suggest that the cellular damage due to magnetic hyperthermia might, indeed, be a very localised phenomenon that, in turn, can activate different cell death mechanisms.

In this scenario, to the best of our knowledge, two main cytotoxic effects induced by magnetic hyperthermia and SPIONs have been suggested: reactive oxygen species (ROS) generation and lysosomal membrane permeabilisation (LMP).

The origin of the production of ROS in cells treated with SPIONs has not yet been fully elucidated. Depending on their concentration and surface chemistry, SPIONs alone (without AMF stimulation) can induce ROS generation; this phenomenon is often used to explain their toxicity at high concentrations.[79] SPION-mediated ROS generation can be due to different mechanisms. When SPIONs are localised in lysosomes, their enzymatic degradation produces the release of iron ions into the cytosol; these ions can, then, participate in the Fenton reaction, where Fe^{3+} and Fe^{2+} catalyse the conversion of hydrogen peroxide (H_2O_2) to hydroxyl or superoxide radicals.[80] In some cases, the SPION surface itself can catalyse this reaction.[81] Other sources of ROS generation in cells after treatment with SPIONs might be linked to potential damage of the mitochondrial membrane;[82] in fact, mitochondrial dysfunction has been associated with an increased cytosolic ROS production.[83] Another proposed mechanism of ROS generation is related to the interaction between SPIONs and NADPH oxidase in the plasma membrane during SPIONs' internalisation.[84]

Obviously, the production of ROS in the presence of SPIONs raises some concerns regarding their biocompatibility. However, there are some considerations to keep in mind when using SPION-mediated magnetic hyperthermia as an anti-cancer approach.

(1) Cells have their natural antioxidant defence, and high concentrations of ROS are necessary to overcome this protective barrier. The concentrations of SPIONs needed to elicit significant oxidative stress are usually higher than those used to trigger magnetic hyperthermia.

(2) ROS generation from SPIONs depends on their surface chemistry and coating, and it has been shown that bare nanoparticles produce a higher ROS amount than coated ones;[82] therefore, SPION coating or encapsulation in nanostructures should significantly lower this effect. Moreover, as already seen in the previous section, a proper targeting of SPIONs to the desired tissue should enhance their accumulation in cancer cells, with minimal or even negligible impact on healthy tissues.

(3) Since the Fenton reaction depends on H_2O_2, ROS production *via* this pathway depends on cell metabolism. Interestingly, since cancer cell metabolism is faster than that of normal cells, they usually have a higher intracellular H_2O_2 concentration;[85] therefore, the Fenton reaction in cancer cells should be more efficient and faster.

Mesárošová *et al.* measured the production of ROS with surface-modified magnetite nanoparticles (magnetite core ≈ 8 nm) in A549 human lung adenocarcinoma and HEL 12469 human embryonic lung fibroblasts and they observed a low but significant intracellular ROS generation in both cell types. Nevertheless, there was no oxidative damage to DNA with respect to control cells; therefore, the ROS produced did not play a significant role in nanoparticle genotoxicity.[82] In this work, however, the effects of the AMF stimulation were not considered. In other studies, authors reported a higher ROS generation upon AMF stimulation of SPIONs. For example, Sola-Leyva *et al.* studied ROS generation in HepG2 human hepatoma cells induced by the stimulation of biomimetic magnetic nanoparticles (BMNPs) with AMF.[86] Results showed that intracellular ROS production was high only in cells incubated with BMNPs + AMF stimulation, while ROS production was not observed in cells treated with BMNPs alone. Similar results were also found in other works.[87,88] The reason why the AMF stimulus enhances ROS production is still unclear. One hypothesis is that the increase in temperature in proximity to the nanoparticle might boost the kinetics of the Fenton reaction.[89] The higher temperature might also alter cell physiology, with consequent ROS production.[90] Another possible mechanism involves initial damage at the level of mitochondria that, in turn, produces ROS as a response; this possibility seems to be more important in systems where the rise in temperature by AMF stimulation is negligible.[86]

The other mechanism responsible for the cytotoxicity of SPION-induced magnetic hyperthermia is known as lysosomal membrane permeabilisation (LMP). Lysosomes are intracellular organelles, the function of which is to "digest" nutrients that the cell acquires from the extracellular environment or to degrade cellular components that are altered or not necessary to the cell anymore. For this reason, lysosomes contain several hydrolytic enzymes with a maximal enzymatic activity at acidic pH, as that found in the lysosome milieu (4.5–5.0).[91,92] When the lysosomal membrane is damaged, these enzymes are released into the cytosol, with potential degradation of vital cellular components, and consequent induction of cell apoptosis. If the damage is important, the cytosol might also experi-

ence a quick acidification, with consequent cell necrosis. Therefore, the extent of the lysosomes' damage drives cell death preferentially towards apoptosis or necrosis.[91] In LMP, only those enzymes that can work at neutral pH for a sufficient amount of time, such as cathepsin B, D or L, for instance,[91] are involved in the activation of apoptotic pathways. Once cathepsins are released into the cytosol, several pathways can induce cell death. Cathepsin B, for instance, has been shown to directly induce nuclear damage. Moreover, both cathepsin B and D can activate caspase-dependent apoptosis thanks to their ability to cleave the protein Bid (BH3-interacting domain death agonist), a member of the Bcl-2 family of proteins that regulate the permeabilisation of the outer mitochondrial membrane. Cleaved-Bid, in fact, binds to Bax that, in turn, associates with the outer mitochondria membrane, forming an oligomeric pore that releases cytochrome c from mitochondria, with consequent activation of caspases.[91] In this sense, cathepsin B has been suggested to mimic the activity of caspase 8.[93] LMP can be triggered by several stresses, such as a high production of ROS near the lysosomal membrane or treatment with some lysosomophilic detergents.[91] Researchers have shown that also SPIONs, activated by AMF, can induce LMP; high concentrations of SPIONs within lysosomes can produce "hot spots" upon AMF stimulation that damage or permeabilise the lysosomal membrane. On the other hand, as previously stated, Fenton reactions facilitated by the AMF stimulus might produce enough ROS to trigger LMP. Domenech et al. demonstrated that IONPs, functionalised to target cancer cells overexpressing the epidermal growth factor receptor, could selectively induce LMP upon stimulation with the AMF.[94] In fact, after magnetic hyperthermia, an increased cathepsin B cytosolic activity was observed. Contextually, authors observed a higher production of ROS, which were considered responsible for the induction of LMP. Interestingly, Sanchez et al. demonstrated that LMP was induced in in vitro endocrine tumours with iron oxide nanocrystals internalised in lysosomes, even at small concentrations (2.2 pg$_{Fe}$ per cell) and with very low thermal power upon AMF stimulation.[95] These results, again, demonstrate that in order to induce a toxic effect on cancer cells, a measurable and global rise in temperature in the cell culture media is not necessary, because a very local heat is enough to trigger cell death. Along this line, one of our recent works also demonstrated that LMP is one of the most plausible mechanisms of cell death induced by magnetic hyperthermia. In our research, we studied the anticancer efficacy of lipid magnetic nanovectors (LMNVs) loaded with SPIONs (3 nm) and with an anticancer drug, nutlin-3a, against an in vitro model of glioblastoma multiforme.[96] The nanocarriers were efficiently taken up by lysosomes that were, in turn, permeabilised during the AMF stimulation, with consequent release of cathepsin B (Fig. 3), suggesting LMP. At the same time, however, no overexpression of HSP 70 was observed after the treatment, suggesting that the global intracellular temperature was not high enough to induce toxicity, whereas a more local heating phenomenon was responsible for LMP induction.
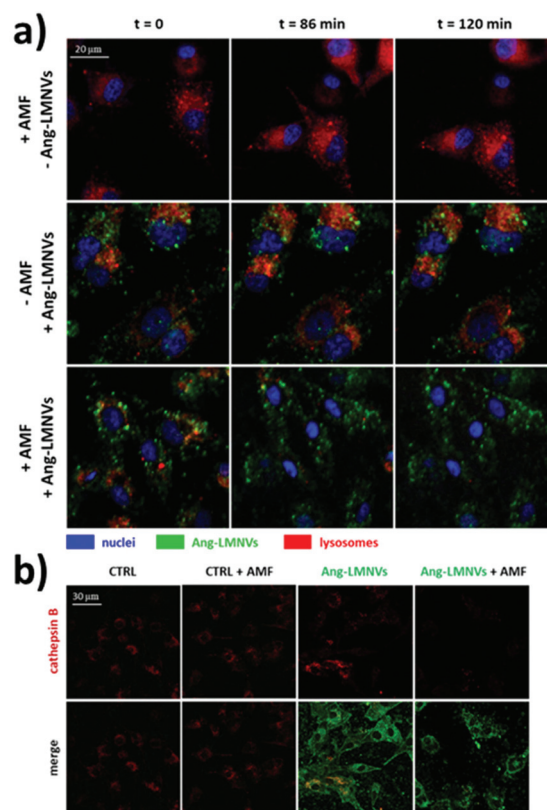

Fig. 3 (a) Representative confocal images at t = 0, 86, and 120 min from the beginning of the stimulation of glioblastoma cells (U87 MG cells) with AMF (16 mT, 753 kHz, for a total of 2 h), incubated with angio-pep2-functionalised lipid magnetic nanovectors (Ang-LMNVs), or stimulated with AMF in the presence of Ang-LMNVs. The time frames were selected from a live confocal acquisition. (b) Cathepsin B confocal imaging (in red) in U87 MG upon different treatments. The loss in fluorescence signal for both lysosomes (stained with LysoTracker Deep Red dye) and cathepsin B (with anti-cathepsin B antibody) is related to LMP. Reproduced with permission from ref. 96. Copyright ACS, 2020.

It is worth noticing that a higher sensitivity of cancer cells towards LMP has been observed, probably due to a slightly different composition and morphology of lysosomes in cancer cells with respect to those present in healthy cells.[92] First of all, cancer cells have a higher concentration of cathepsins. While a higher amount and activity of cathepsins in the extracellular environment contributes to enhanced tumour growth, invasion, and angiogenesis, their higher accumulation in lysosomes (especially of cysteine cathepsins such as cathepsin B) destabilises the lysosomal membrane, making cancer cells more sensitive to stresses and reducing their survival.[92] It has been also demonstrated that larger lysosomes, often found in cancer cells,[97] are also more sensitive to LMP, for reasons that are not entirely clarified.[98] Finally, as previously stated, cancer cells have higher metabolic and ROS generation rates; ROS can also have a negative impact on lysosome stability, making LMP easier in cancer cells.[91] Considering that some apoptotic pathways are often inhibited in cancer cells due to a reduced expression of pro-apoptotic effector molecules or to an over-

expression of anti-apoptotic proteins, LMP is a very promising anticancer approach in apoptosis-resistant cancer cells.

Recent *in vivo* studies were also aimed at investigating SPION-induced magnetic hyperthermia efficacy and understanding its mechanism of action. Jeon *et al.* studied the *in vivo* efficacy of magnetic hyperthermia induced with PEG-coated iron oxide multigranule nanoclusters (PEG-MGNCs) compared to PEGylated single iron oxide nanoparticles (PEG-NPs) in SCC7 (mouse squamous cell carcinoma) tumour-bearing mice.[99] The AMF stimulation (19.5 kA m^{-1}, 389 kHz) was induced after 24 and 48 h from nanoparticles' injection and lasted 30 min. As can be seen from Fig. 4a, at the end of the stimulus, the temperature of the tumour tissue treated with PEG-MGNCs reached $\approx$45 °C. On the other hand, tumours treated with saline solutions (control) and PEG-NPs reached, respectively, 34.8 and 35.2 °C. The more efficient hyperthermia treatment with PEG-MGNCs was correlated with a significant inhibition of the tumour size to a final volume of 328.29 ± 28.56 mm^3 with respect to mice treated with saline solution (1429.7 ± 256.5 mm^3) and PEG-NPs (1418.1 ±

Fig. 4 (a) Thermal image of tumour tissues 24 h after intravenous injection of PEG-NPs and PEG-MGNCs (8 mg kg^{-1}) upon AMF stimulation (19.5 kA m^{-1}, 389 kHz). (b) Inhibition of tumour growth. Samples treated with hyperthermia field (HF) are highlighted with arrows (*$p < 0.05$). (c) Tumour weight after magnetic hyperthermia. (d) Pictures of mice and tumours before and 8 days after magnetic hyperthermia. (e) Hematoxylin and eosin (H&E) staining and (f) immunohistochemistry of HSP 70 in the tumour tissues after 8 days upon treatment with saline, PEG-NPs, PEG-MGNCs, saline + HF, PEG-NPs + HF, and PEG-MGNCs + HF. Reproduced with permission from ref. 99. Copyright ACS, 2020.

214.0 mm^3) plus hyperthermia fields (HF). Moreover, tumours treated with PEG-MGNCs + HF showed the presence of necrotic areas and a higher expression of HSP 70 (Fig. 4e and f). In another work, breast cancer-bearing BALB/c mice were treated with IONPs functionalised with the fourth generation of poly(amidoamine) dendrimers (G4@IONPs) and AMF.[100] The tumour volume in treated mice decreased to 23.7% with respect to the initial tumour volume over 27 days. In control mice, tumour volume reached 448% with respect to the initial value. The tumour growth suppression in treated mice was shown to be a consequence of the inhibition of tumour angiogenesis and of an increased cellular necrosis. More recently, Beola *et al.* studied IONP-induced magnetic hyperthermia in a murine model of pancreatic cancer.[101] On the same day as the nanoparticles' injection, mice were stimulated with an AMF (196 kHz, 26 kA m^{-1}) for 30 min; mice were stimulated also in the following two days. The authors then followed the expression of a marker of immunogenic cell death (ICD) to assess whether the treatment was able to generate an immune response. Cells undergoing death mechanisms might in fact express specific molecules (damage-associated molecular patterns) that, in turn, trigger an immunostimulatory effect. As also explained by the authors, the relocation of calreticulin (CALR) proteins to the outer side of the plasmatic membrane of the cells, induced by caspase-8 activation and other apoptosis signalling molecules, is a clear indicator of the beginning of ICD. Tumours treated with magnetic nanoparticles + AMF had a significantly higher expression of CALR in plasmatic membranes ($\approx$80%), with respect to the control groups ($\approx$15%). Interestingly, the authors showed that tumour tissues treated with magnetic nanoparticles alone (without AMF stimulus) already presented a higher amount of plasmatic CALR ($\approx$55%) with respect to controls; nevertheless, this immunostimulatory effect was not associated with toxicity *in vitro*. Authors also showed that the tumour growth rate in animals treated with magnetic nanoparticles + AMF was reduced with respect to control animals and animals treated just with AMF; however, the outcome was very heterogeneous, with a subgroup of animals where the treatment was less effective. This was demonstrated to be correlated to a lower number of particles internalised in the tumour, and to a higher leakage towards other organs (*e.g.*, liver and spleen). This work clearly demonstrated how the biodistribution of nanoparticles for magnetic hyperthermia strongly affects the treatment efficacy.

Chauhan *et al.* studied the *in vivo* tumour inhibition with chitosan-coated IONPs + AMF, by finding a good balance between safe IONP concentration/AMF conditions and treatment efficacy.[102] The aim was, in fact, to trigger apoptosis instead of necrosis, in order to reduce possible side effects due to a strong response of the immune system induced by necrosis. By choosing AMF conditions below the recommended limit of $H \times f$ and by using relatively low SPION concentrations ($\approx$2 μg mm^{-3}), administered by intratumour injections to reduce nanoparticles' leakage towards other body areas, they were able to achieve tumour removal with temperatures below 45 °C, triggering apoptosis instead of necrosis, with lower side effects.
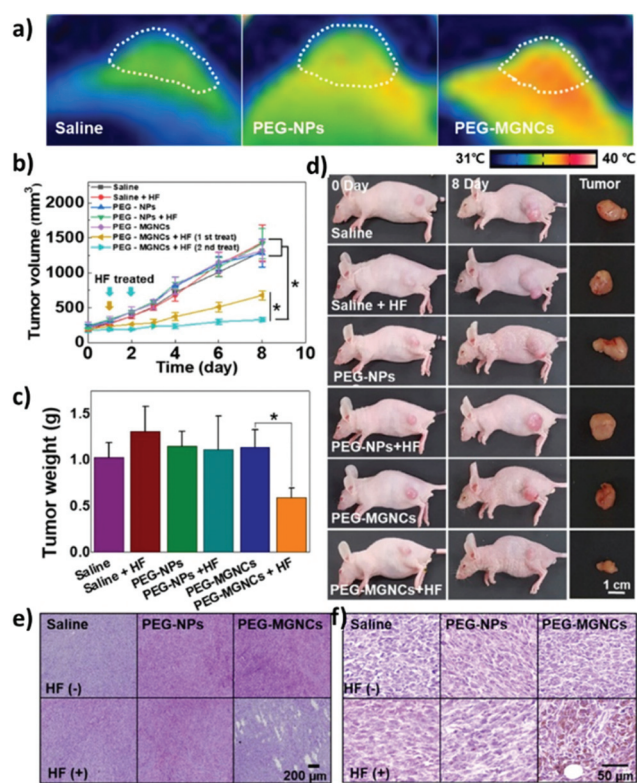
SPIONs and magnetic hyperthermia in the omics era

Omics unveiling cell response to SPIONs/AMFs

In spite of an overall high level of safety attributed to SPIONs (and to iron oxide in general) for the metabolism of animals, multiple groups have raised concerns about possible adverse effects, and some toxicological studies adopted large-scale strategies. The use of SPIONs as MRI contrast agents for clinical stem-cell tracking, for example, has inspired a microarray investigation about the transcriptional impact of SPIONs on C17.2 mouse neural stem cells.[103] The assay, however, did not highlight any sign of major distress, only detecting a transient response from the iron-homeostasis machinery. Conversely, miRNA evaluations on PC12 neuroblasts by Sun *et al.* support SPIONs as neurotoxic, eliciting cell states reminiscent of those found in neurodegenerations.[104]

Potential hazards from SPIONs may in fact stem from several factors – like concentration, synthesis, size, surface features, and cellular context – and this ultimately makes risks difficult to assess for specific applications on the one hand, and research prone to prejudice on the other.[105] When Harris and co-authors systematically tested multiple experimental variables, they could spot significant changes in side effects from iron oxide nanomaterials, such as alterations of apoptotic rates and cell viability. They administered such nanoparticles to growing mouse and monkey fibroblasts, with automated modalities for culturing, imaging, and DNA fragmentation/oxidation analysis.[106] While the study was mostly concerned with the optimisation of a fast methodology to evaluate the noxious potential of nanoparticles, it certainly shows the importance of contingent determinants affecting iron oxide nanoparticle safety, and testifies the validity of high-throughput approaches to appreciate complex patterns of toxicity.

The relevancy of nanoparticle size for toxicity was also stressed by a transcriptomic comparison between L02 human hepatocytes treated with either ultra-small or regular SPIONs.[107] A reduced average diameter was sufficient to increase hepatotoxicity, specifically promoting acute inflammation and by altering endoplasmic reticulum stability.

Intrinsic toxicity was detectable in a proteomics dataset – reported by us[74] – involving LMNVs loaded with SPIONs and functionalised with an antibody against the transferrin receptor (TfR). The experiment tested the impact of such vectors in three-dimensional cell cultures of U87 glioblastoma multiforme, in the presence or absence of AMF and with or without the antitumoural drug temozolomide. The investigation yielded lists of proteins virtually justifying apoptotic/necrotic phenotypes, especially when LMNVs and AMF were co-administered. Although with relevant variations, nevertheless, LMNVs changed protein composition in all experimental circumstances we explored (Fig. 5). Some inherent toxicity from them cannot be ruled out, at least to some extent, but it should be taken into account that a precise tuning of dosages was beyond the goals of the study, and remains highly dependent on setup. The observed phenomena, in sum, may have been largely owing to peculiarities of our nanoparticles, experimental design, or *in vitro* platform.

Omics for the characterisation of biological modifications on SPIONs

Not only can omics strategies inform about changes in the biological environment of SPIONs, but they can also provide detailed information about the nanoparticle–organism inter-
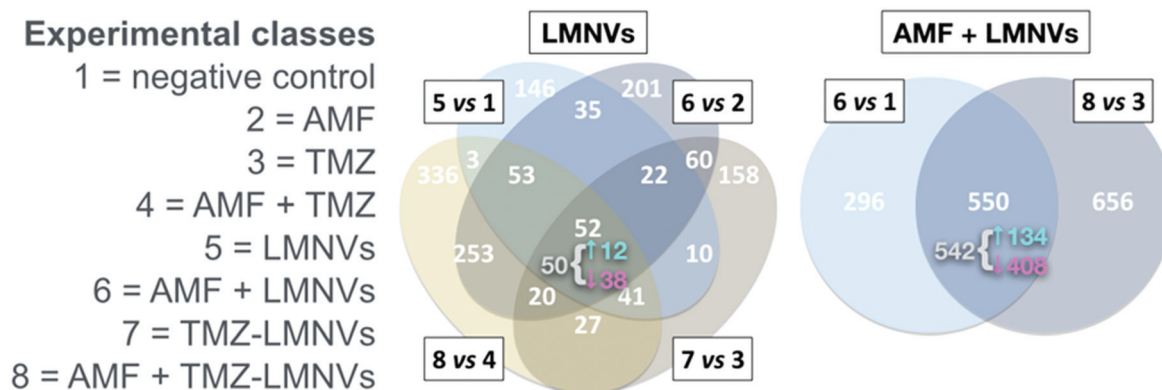

Fig. 5   Impact of SPION-loaded LMNVs, with or without AMF, on the proteome of a glioblastoma multiforme model. Experimental classes are listed on the left. TMZ = temozolomide. Venn diagrams show the impact of LMNVs alone (center) or the combination of LMNVs and AMF (AMF + LMNVs, right) on protein composition. Comparisons between couples of experimental classes are represented as sets (ovals or circles) of differentially represented proteins (DRPs). At each subset, the number of DRPs shared by the relevant parent sets is shown. For both Venn diagrams, at the intersection of all parent sets, we report (in grey) the fraction of DRPs that is coherent, meaning the proportion of proteins being systematically either up- or down-regulated in all parent sets. The sub-fractions of up-regulated coherent DRPs (↑, in cyan) and down-regulated DRPs (↓, in magenta) are also indicated (next to a brace). In this dataset, LMNVs show a comparatively major influence *per se* on the proteome, but the number of DRPs becomes even higher when AMF and LMNVs are both administered, consistent with the presence of synergies between the two experimental variables. Reproduced and adapted with permission from ref. 74. Copyright Royal Society of Chemistry, 2019.

face.[108] Protein coronas, for instance, have received considerable attention because of their great impact on nanoparticle toxicity, permeability, clearance, and the like.[109] The outermost regions of a SPION are, understandably, critical in determining the type of protein corona that builds up on it upon contact with biological fluids. By means of proteomics, a study evaluated variations in protein composition within protein coronas of silica- *vs.* dextran-coated SPIONs, after incubation in plasma. Systematic differences were found between the two particle types for several classes of plasma proteins, *e.g.*, those regulating coagulation. Compared to non-incubated SPIONs, silica- and dextran-associated protein coronas each imparted unique features to plasma-exposed SPIONs when given to human macrophages, such as in terms of biocompatibility and internalisation rates.[110]

Dextran-coated SPIONs in blood had already been studied *via* proteomics in an investigation by Simberg and colleagues.[111] Again, differences in protocols for nanoparticle incubation and methods for biological testing might account for the relevant dissimilarities in the identity of proteins indicated as components of dextran-associated coronas. Still, the two groups agree on the fact that the dextran-elicited protein corona does not participate in particle uptake from macrophages. Possibly, a specific interaction between SPION cores and macrophage membrane receptors takes place, either through iron-binding or dextran-binding domains.

SPIONs for omics technologies

Depending on their synthesis and subsequent modifications, magnetic nanoparticles can be rendered capable of binding to specific classes of biomolecules, or even to selectively attach to single targets, such as a given peptide. This characteristic, combined with their responsiveness to externally applied magnetic fields, makes them particularly apt to execute fine and customisable molecular work. Theoretical applications span from conditional or spatially confined reactions – *e.g.*, for drug delivery, local heating, or enzymatic catalysis – to iteration of tasks.

Magnetic nanoparticles, for instance, have already been proposed as key components for the semi-automation of a biopanning process of antibody libraries, namely the operation of selecting high-affinity antibodies from an initially diverse pool. Phage display is a large-scale screening technique to discover protein–protein interactions; it exploits a population of bacterial viruses (phages), differing from one another just by a gene, the product of which is also exhibited on the surface of the phage. Such a population can be exposed to an antigen of interest, and only those individuals bearing a high-affinity outer protein – in our case an antibody – will bind to the antigen with sufficient strength to endure a series of washes.[112,113] Normally, this means that only the most promising antibodies against a single molecule are retained, and that other molecules that might have been valuable for further antigens are simply swept away. When phages are bound to magnetic nanoparticles, in turn, multiple antigens can have their antibodies identified from a single library. Several wells, each

containing a different antigen, are serially treated with the same phage library, and unbound viruses are magnetically recovered at every step through a magnetic particle processor system, with a dramatic increment in both efficiency and efficacy of the whole procedure.[114]

Compared to other types of magnetic nanoparticles, the biocompatibility of SPIONs and their usability to induce local hyperthermia offer even more advantages in high-throughput biotechnologies. Fully biocompatible arrays of micro test tubes/beakers made of silicon and coated with SPIONs have been proposed as biosensors for large-scale analyses: authors thought they could use them to land SPION-attached, *ad hoc*-designed nucleic acids to specific areas of the substrate. By repeating the process for a desired number of sequences of interest, one would obtain an analogue of a microarray, such as those utilised for genomics.[115] Nanoconjugates of SPIONs with artificial nucleic acids exist, and these could be appropriate for specific microarray uses, *e.g.*, those requiring a particularly long shelf-life, high sensitivity to single-nucleotide polymorphisms, or enhanced detectability of long DNA stretches.[33,116] More different implementations are easily imaginable: peptides could be docked in a similar way, either for proteomics, diagnostics, interaction studies, and so forth. Specific reactions may be carried out in single pores, and temperatures could be modulated at precise coordinates, with micrometric precision.

Blume *et al.* characterised the plasma proteome by optimising a proteomics pipeline and gathering data from the protein corona of nanoparticles recovered from plasma. They screened 43 kinds of SPIONs, selecting those yielding proteins more effectively.[117] With respect to other nanoparticles, SPIONs were considered to be particularly promising to capture plasma proteins *in vitro* for downstream proteomics, due to their favourable surface characteristics, and because they can be retrieved swiftly with a magnet. Protein coronas on SPIONs mostly depend on outer modifications and, all things considered, these formations are not solely interesting to figure out interactions of SPIONs with biological systems, yet they may also be useful to probe the environments to which SPIONs have been exposed.

An area of omics for which SPION-based strategies have proved their soundness is subcellular omics. The field aims at identifying the internal composition of sets of biological molecules within cellular compartments. With a proper design and coating, SPIONs can capture a desired organelle. An example comes from Tharkeshwar and colleagues, who used aptly made magnetically driven SPIONs with different coatings to bind and isolate different cell components, and conducted extensive analyses – including omics – to assess biological variations between populations of HeLa human cervical cancer cells, namely wild-type *vs.* Niemann–Pick disease type C1 (NPC1)-deficient ones.[118] An absent or non-functional NPC1 has a negative impact on the intracellular distribution of cholesterol. From cell homogenates, the team enriched for plasma membrane using aminolipid-coated SPIONs, and for late endosomes/lysosome with DMSA-SPIONs. On both frag-

ments (plus total lysates as references), they performed lipidomics and proteomics, which helped to decipher the cytological bases of the pathogenic phenotype brought by the NPC1 knockout: mutants displayed relatively unaltered cytoplasmic membrane, while presenting severely impaired trafficking at the lysosome level. The experiment, therefore, demonstrates that the approach can improve our understanding of subcellular dynamics, with potentially important repercussions in biomedicine.

Other studies validated the use of SPIONS to segregate cellular components, with some emphasis on lysosomes.[119] At present, mature lysosome-purification protocols for multiple omics aided by SPIONS are available.[120] With the advent of single-cell omics, the omics branch taking individual cells as input, SPIONS may be among those tools leading to an *avant-garde* dissection of molecular mechanisms. They could, in brief, offer a means to couple single-cell analyses with organelle isolation, perhaps playing a part in the rise of single-organelle omics.

Clinical advances of SPIONs and magnetic hyperthermia

From the 1950s, articles on hyperthermia for cancer therapy started to be published; nevertheless, interest in this topic started to grow from the 1970s, when the first clinical trials began to give encouraging results. The attention towards magnetic hyperthermia, and in particular towards SPIONS as means to induce hyperthermia in cancer cells, is quite recent; in fact, clinical studies in humans only started in 2006 and they still represent a small fraction of the studies on hyperthermia in general (Fig. 6).

In 2006, Wust *et al.* performed a one-armed feasibility study involving 22 subjects suffering from recurrences of different tumours.[121] The magnetic nanoparticles used in this study were aminosilane-coated SPIONS (15 nm) dispersed in water. Depending on the typology of the tumour, aminosilane-coated SPIONS were injected in different ways: computed tomography (CT)-guided infiltration for 6 patients with sarcoma, cervical

and ovarian carcinoma, and cancer of the rectum (group A); transperineal injection for 8 patients with prostate carcinoma after definitive radiotherapy (group B); intraoperative administration under visual control after resection for 8 patients with cervical carcinoma (group C). The administration of SPIONS was well tolerated by all groups, with only a few side effects reported. Depending on the body area, different magnetic field strengths were used (3.0–6.0 kA m^{-1} in the pelvis, up to 7.5 kA m^{-1} in the thoracic and neck region and >10.0 kA m^{-1} for the head), obtaining a SAR of 60–380 W kg^{-1} in the target, with an AMF frequency of 100 kHz. However, only 30% of the target volume in group A and 0.2% in group B reached a temperature ≥42 °C, suggesting that improvements in the treatment protocol are necessary.[121] In another study by Maier-Hauff *et al.*, the feasibility and tolerability of thermotherapy induced by magnetic nanoparticles (aminosilane-coated SPIONS) combined with external beam radiotherapy was demonstrated in 14 patients with glioblastoma multiforme.[122] The patients were exposed to an AMF of 100 kHz and strength varying from 2.5 to 18 kA m^{-1} for a median of 6 treatments following administration of SPIONS, and to single fractions (2 Gy) of a radiotherapy series of 16–70 Gy. Also this study demonstrated the tolerability of thermotherapy with SPIONS, reaching median maximum intratumoural temperatures of 44.6 °C. Later, the same research group conducted a clinical trial that showed that patients with glioblastoma multiforme (mostly recurrent) treated with SPIONS and AMF had longer overall survival following diagnosis of first tumour recurrence (13.4 months) and overall survival after primary tumour diagnosis (23.2 months), with respect to reference groups that did not receive this kind of treatment (6.2 and 14.6 months, respectively).[123] Results from a clinical trial concerning thermotherapy of locally recurrent prostate cancer with SPIONS were also published by Johannsen *et al.* in 2007.[124] In this study, the intratumour temperature was followed in 10 patients, previously treated with SPIONS (transperineal administration) and then exposed to AMF 6 times, 60 min each, at weekly intervals. Results showed that maximum temperatures up to 55 °C were achieved in the prostate. Median temperatures in 20%, 50%, and 90% of the prostate were 41.1 °C, 40.8 °C, and 40.1 °C, respectively,
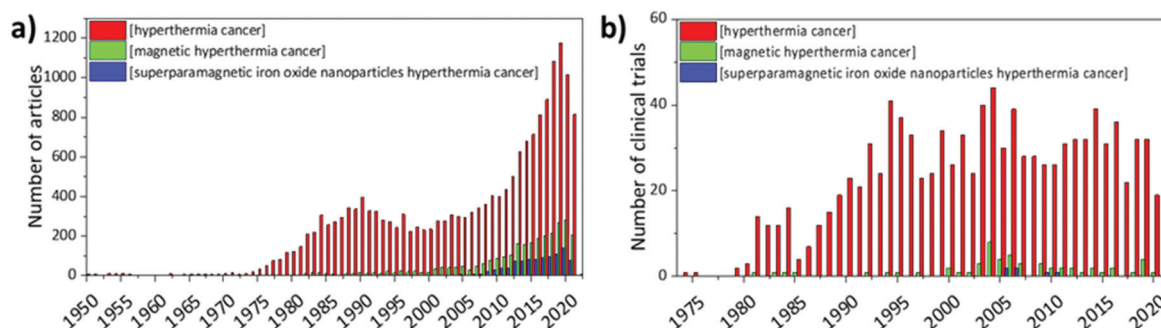

Fig. 6 (a) Number of articles and (b) number of clinical trials published until 2021. Data were exported from PubMed (https://pubmed.ncbi.nlm.nih.gov/), using the search terms "hyperthermia cancer" (red), "magnetic hyperthermia cancer" (green), and "superparamagnetic iron oxide nanoparticles hyperthermia cancer" (blue).

with a median thermal dose of 7.8 cumulative equivalent minutes at 43 °C in 90% of the prostate.

Two clinical studies concerning SPIONs and magnetic hyperthermia are also currently present in the clinicaltrial.gov database (search terms "cancer; superparamagnetic iron oxide nanoparticles"). In particular, a phase 0 clinical trial (NCT02033447) aims at evaluating the retention and maintenance of SPIONs in the prostate after injection in patients that need to undergo prostatectomy. This will give important information about the actual concentration of magnetic nanoparticles in the injection site before AMF stimulation and their potential distribution to other neighbouring sites. This trial was first posted in 2014 and the "recruitment status" appears as "complete"; however, there are still no available results.[125] Another recent phase I clinical trial posted in 2020 and not yet recruiting will study the safety, efficacy, and tolerability of SPIONs with spinning magnetic fields (SMF) in combination with neoadjuvant chemotherapy in patients with osteosarcoma (NCT04316091).[126] In this case, however, the physical rotation and vibration of the SPIONs, triggered by the stimulation with a new type of magnetic field generated by the spinning of a cylindrical magnet along its axis, is exploited.

It must be stressed, however, that there are currently several clinical trials involving the potential use of SPIONs as MRI contrast agents. The current limitations of magnetic hyperthermia triggered by SPIONs depend on several aspects. From a practical point of view, as pointed out by Maier-Hauff *et al.*,[123] stimulation with magnetic fields presents the drawback that all metal implants within 40 cm of the treatment area must be removed for the safety of the patient. Moreover, due to the strong interactions between SPIONs and magnetic fields, and the relatively high concentrations of SPIONs necessary to induce a significant increase in temperature in the treatment area, tumour progression cannot be followed with MRI due to artefacts related to the presence of the magnetic nanoparticles. Nevertheless, other imaging techniques such as CT, positron emission tomography (PET) and single-photon emission computed tomography (SPECT) could be used.[123] Another fundamental aspect that has been already raised in the previous sections is the lack of clear understanding of the mechanisms behind the anticancer effect of magnetic hyperthermia. Only with a strong view of the heating mechanism (if any) and of the anticancer action will researchers be able to improve the efficacy of the approach and make SPION-induced magnetic hyperthermia a standard of care.

Conclusions

SPION-mediated magnetic hyperthermia offers a promising alternative to conventional anticancer approaches. In fact, the functionalisation of the SPION surface with biocompatible coatings, and the possibility to attach functional ligands that can specifically target diseased tissues, make them a very interesting system to trigger magnetic hyperthermia. The interaction between SPIONs and AMF is able to produce a very loca-

lised heat that can damage cellular components or foster the production of toxic agents that, in turn, induce the activation of cell death mechanisms. In this review, we have shown that the anticancer action of SPION-induced magnetic hyperthermia can be activated by several mechanisms, depending on particle features and concentration, on intracellular localisation, and on cell type. Most of the *in vitro* and *in vivo* studies show possible effects due to the high temperatures reached within the cell (protein unfolding, nuclear damage, plasma membrane permeabilisation) or to confined heating phenomena that induce ROS generation and lysosomal membrane permeabilisation. SPIONs are also becoming more and more important in omics technologies, where their features could be exploited to understand molecular mechanisms at single-cell levels.

Summarising, the use of SPIONs in magnetic hyperthermia offers several advantages with respect to other systems. First of all, their superparamagnetic properties make their heating capacities superior to ferromagnetic bulk materials, and their null remanent magnetisation prevents their aggregation in biological media. Thanks to their magnetic properties, SPIONs can be guided to the diseased area by applying an external magnetic field: this guarantees a higher accumulation within the region of interest, improving efficacy and reducing side effects, and is even more convenient when IONPs are co-delivered with drugs.[127,128] Effective coatings and functionalisation strategies allow cancer cells to be specifically targeted, with a precision at the cellular level. A considerable amount of research is focused on tailoring the surface of SPIONs and of their nanocomposites with biological molecules that can interact with specific receptors on target cells; this strategy can deliver nanocarriers to deep-seated tumours, providing localized hyperthermia, and preventing damage to healthy tissues.[129] Despite all these advantages, there are still some key aspects that need to be addressed in order to improve SPION-mediated magnetic hyperthermia and facilitate its clinical translation. For instance, improved targeting strategies with patient specificity would significantly reduce non-specific heating and increase efficacy, even in tumours with high genetic heterogeneity. SPIONs' physicochemical properties should be tailored in order to enhance antitumour effects at lower magnetic field strength, increasing the tolerability of the treatment by the human body and improving efficacy also for deep-seated tumours.[130–132] Furthermore, in order to optimize clinical magnetic hyperthermia treatment, there are studies focused on computer-aided hyperthermia treatment preoperative plans, which can improve the efficiency and the safety of the treatment.[133,134] Finally, a clear understanding of the mechanisms at the base of the antitumour activity of SPION-mediated magnetic hyperthermia would surely boost their exploitation in clinical practice.

Author contributions

CP, AD, MBG: conceptualisation; writing, original draft. GC: conceptualisation; writing, review & editing; funding acquisition.

Conflicts of interest

There are no conflicts to declare.

Acknowledgements

References

1 J. Overgaard, *Cancer*, 1977, **39**, 2637–2646.
2 R. T. Gordon, J. R. Hines and D. Gordon, *Med. Hypotheses*, 1979, **5**, 83–102.
3 S. L. Brown, J. W. Hunt and R. P. Hill, *Int. J. Hyperthermia*, 1992, **8**, 501–514.
4 A. Hervault and N. T. K. Thanh, *Nanoscale*, 2014, **6**, 11553–11573.
5 S. Dutz and R. Hergt, *Int. J. Hyperthermia*, 2013, **29**, 790–800.
6 E. A. Périgo, G. Hemery, O. Sandre, D. Ortega, E. Garaio, F. Plazaola and F. J. Teran, *Appl. Phys. Rev.*, 2015, **2**, 041302.
7 A. Neuwelt, N. Sidhu, C. A. A. Hu, G. Mlady, S. C. Eberhardt and L. O. Sillerud, *Am. J. Roentgenol.*, 2015, **204**, W302–W313.
8 H. Wei, O. T. Bruns, M. G. Kaul, E. C. Hansen, M. Barch, A. Wiśniowska, O. Chen, Y. Chen, N. Li, S. Okada, J. M. Cordero, M. Heine, C. T. Farrar, D. M. Montana, G. Adam, H. Ittrich, A. Jasanoff, P. Nielsen and M. G. Bawendi, *Proc. Natl. Acad. Sci. U. S. A.*, 2017, **114**, 2325–2330.
9 X. Yin, S. E. Russek, G. Zabow, F. Sun, J. Mohapatra, K. E. Keenan, M. A. Boss, H. Zeng, J. P. Liu, A. Viert, S. H. Liou and J. Moreland, *Sci. Rep.*, 2018, **8**, 1–10.
10 L. Zhu, Z. Zhou, H. Mao and L. Yang, *Nanomedicine*, 2017, **12**, 73–87.
11 A. J. Gauger, K. K. Hershberger and L. M. Bronstein, *Front. Chem.*, 2020, **8**, 561.
12 A. S. Thakor, J. V. Jokerst, P. Ghanouni, J. L. Campbell, E. Mittra and S. S. Gambhir, *J. Nucl. Med.*, 2016, **57**, 1833–1837.
13 R. M. Cornell and U. Schwertman, *The Iron Oxides*, New York, 2003.
14 M. A. Vergés, R. Costo, A. G. Roca, J. F. Marco, G. F. Goya, C. J. Serna and M. P. Morales, *J. Phys. D: Appl. Phys.*, 2008, **41**, 134003.
15 S. M. Devi, A. Nivetha and I. Prabha, *J. Supercond. Novel Magn.*, 2019, **32**, 127–144.
16 C. L. Dennis and R. Ivkov, *Int. J. Hyperthermia*, 2013, **29**, 715–729.
17 S. Tanwar, V. P. S. Awana, S. P. Singh and R. Pasricha, *J. Supercond. Novel Magn.*, 2012, **25**, 2041–2045.
18 W. J. Atkinson, I. A. Brezovich and D. P. Chakraborty, *IEEE Trans. Biomed. Eng.*, 1984, **BME-31**, 70–75.
19 J. P. Fortin, F. Gazeau and C. Wilhelm, *Eur. Biophys. J.*, 2008, **37**, 223–228.
20 C. Naud, C. Thébault, M. Carrière, Y. Hou, R. Morel, F. Berger, B. Diény and H. Joisten, *Nanoscale Adv.*, 2020, **2**, 3632–3655.
21 Y. I. Golovin, D. Y. Golovin, K. Y. Vlasova, M. M. Veselov, A. D. Usvaliev, A. V. Kabanov and N. L. Klyachko, *Nanomaterials*, 2021, **11**, 2255.
22 M. Kermanian, S. Sadighian, A. Ramazani, M. Naghibi, M. Khoshkam and P. Ghezelbash, *ACS Biomater. Sci. Eng.*, 2021, **7**, 2701–2715.
23 F. Senturk, S. Cakmak, I. C. Kocum, M. Gumusderelioglu and G. G. Ozturk, *Colloids Surf., A*, 2021, **622**, 126648.
24 E. Halevas, B. Mavroidi, C. M. Nday, J. Tang, G. C. Smith, N. Boukos, G. Litsardakis, M. Pelecanou and A. Salifoglou, *J. Inorg. Biochem.*, 2020, **213**, 111271.
25 C. Y. Yeh, J. K. Hsiao, Y. P. Wang, C. H. Lan and H. C. Wu, *Biomaterials*, 2016, **99**, 1–15.
26 M. Soleymani, M. Velashjerdi, Z. Shaterabadi and A. Barati, *Carbohydr. Polym.*, 2020, **237**, 116130.
27 V. M. Wu, E. Huynh, S. Tang and V. Uskoković, *Acta Biomater.*, 2019, **88**, 422–447.
28 R. A. Puiu, P. C. Balaure, E. Constantinescu, A. M. Grumezescu, E. Andronescu, O. C. Oprea, B. S. Vasile, V. Grumezescu, I. Negut, I. C. Nica and M. S. Stan, *Pharmaceutics*, 2021, **13**, 1356.
29 J. G. Ovejero, D. Cabrera, J. Carrey, T. Valdivielso, G. Salas and F. J. Teran, *Phys. Chem. Chem. Phys.*, 2016, **18**, 10954–10963.
30 M. Zuvin, M. Koçak, Ö. Ünal, Y. Akkoç, Ö. Kutlu, H. Yağci Acar, D. Gözüaçik and A. Koşar, *J. Magn. Magn. Mater.*, 2019, **483**, 169–177.
31 F. Vurro, Y. Jabalera, S. Mannucci, G. Glorani, A. Sola-Leyva, M. Gerosa, A. Romeo, M. G. Romanelli, M. Malatesta, L. Calderan, G. R. Iglesias, M. P. Carrasco-Jiménez, C. Jimenez-Lopez and M. Perduca, *Nanomaterials*, 2021, **11**, 766.
32 M. P. Nguyen, M. H. Nguyen, J. Kim and D. Kim, *Eur. Polym. J.*, 2020, **122**, 109396.
33 M. Galli, A. Guerrini, S. Cauteruccio, P. Thakare, D. Dova, F. Orsini, P. Arosio, C. Carrara, C. Sangregorio, A. Lascialfari, D. Maggioni and E. Licandro, *RSC Adv.*, 2017, **7**, 15500–15512.
34 Y. Patil-Sen, E. Torino, F. De Sarno, A. M. Ponsiglione, V. Chhabria, W. Ahmed and T. Mercer, *Nanotechnology*, 2020, **31**, 375102.
35 S. De Vincentiis, A. Falconieri, F. Mickoleit, V. Cappello, D. Schüler and V. Raffa, *Int. J. Mol. Sci.*, 2021, **22**, 4126.
36 S. Kaushik, J. Thomas, V. Panwar, H. Ali, V. Chopra, A. Sharma, R. Tomar and D. Ghosh, *ACS Appl. Bio Mater.*, 2020, **3**, 779–788.
37 M. Galli, B. Rossotti, P. Arosio, A. M. Ferretti, M. Panigati, E. Ranucci, P. Ferruti, A. Salvati and D. Maggioni, *Colloids Surf., B*, 2019, **174**, 260–269.

38 L. Gutiérrez, L. De La Cueva, M. Moros, E. Mazarío, S. De Bernardo, J. M. De La Fuente, M. P. Morales and G. Salas, *Nanotechnology*, 2019, **30**, 112001.

39 X. Yan, G. Han, S. Wang, C. Chong, D. Han, J. Tan and B. Zhang, *Mater. Chem. Phys.*, 2021, **260**, 124108.

40 S. Ghosh, I. Ghosh, M. Chakrabarti and A. Mukherjee, *Food Chem. Toxicol.*, 2020, **136**, 110989.

41 B. Mol, A. E. Beeran, P. S. Jayaram, P. Prakash, R. S. Jayasree, S. Thomas, B. Chakrapani, M. R. Anantharaman and M. J. Bushiri, *J. Mater. Sci. Mater. Med.*, 2021, **32**, 1–14.

42 Z. Tang, Y. Zhou, H. Sun, D. Li and S. Zhou, *Eur. J. Pharm. Biopharm.*, 2014, **87**, 90–100.

43 A. N. Dizaji, M. Yilmaz and E. Piskin, *Artif. Cells, Nanomed., Biotechnol.*, 2016, **44**, 1109–1115.

44 G. S. Ningombam, D. Chattopadhyay, K. Sarkar, S. N. Kalkura and N. R. Singh, *Colloids Surf., A*, 2021, **625**, 126826.

45 E. C. S. Santos, J. A. Cunha, M. G. Martins, B. M. Galeano-Villar, R. J. Caraballo-Vivas, P. B. Leite, A. L. Rossi, F. Garcia, P. V. Finotelli and H. C. Ferraz, *J. Alloys Compd.*, 2021, **879**, 160448.

46 F. Chen, C. Li, Y. Zhu, X. Zhao, B. Lu and J. Wu, *Biomater. Sci.*, 2013, **1**, 1074–1081.

47 M. Azhdarzadeh, F. Atyabi, A. A. Saei, B. S. Varnamkhasti, Y. Omidi, M. Fateh, M. Ghavami, S. Shanehsazzadeh and R. Dinarvand, *Colloids Surf., B*, 2016, **143**, 224–232.

48 Q. Lu, X. Dai, P. Zhang, X. Tan, Y. Zhong, C. Yao, M. Song, G. Song, Z. Zhang, G. Peng, Z. Guo, Y. Ge, K. Zhang and Y. Li, *Int. J. Nanomed.*, 2018, **13**, 2491–2505.

49 T. T. H. Thi, E. J. A. Suys, J. S. Lee, D. H. Nguyen, K. D. Park and N. P. Truong, *Vaccines*, 2021, **9**, 359.

50 O. Bixner and E. Reimhult, *J. Colloid Interface Sci.*, 2016, **466**, 62–71.

51 M. Yusefi, K. Shameli, O. S. Yee, S. Y. Teow, Z. Hedayatnasab, H. Jahangirian, T. J. Webster and K. Kuča, *Int. J. Nanomed.*, 2021, **16**, 2515–2532.

52 A. Singh, S. Jain and S. K. Sahoo, *Mater. Sci. Eng., C*, 2020, **110**, 110695.

53 A. Adamiano, V. M. Wu, F. Carella, G. Lamura, F. Canepa, A. Tampieri, M. Iafisco and V. Uskoković, *Nanomedicine*, 2019, **14**, 1267–1289.

54 J. G. Ovejero, D. Cabrera, J. Carrey, T. Valdivielso and G. Salas, *Phys. Chem. Chem. Phys.*, 2016, **18**, 10954–10963.

55 M. Yusefi, K. Shameli, O. S. Yee, S.-Y. Teow, Z. Hedayatnasab, H. Jahangirian, T. J. Webster and K. Kuča, *Int. J. Med.*, 2021, **16**, 2515–2532.

56 F. Senturk, S. Cakmak, I. Cengiz and M. Gumusderelioglu, *Colloids Surf., A*, 2021, **622**, 126648.

57 E. Halevas, B. Mavroidi, C. M. Nday, J. Tang, G. C. Smith, N. Boukos, G. Litsardakis, M. Pelecanou and A. Salifoglou, *J. Inorg. Biochem.*, 2020, **213**, 111271.

58 G. Singh, D. Chattopadhyay and K. Sarkar, *Colloids Surf., A*, 2021, **625**, 126826.

59 Y. Sun, H. S. Kim, J. Park, M. Li, L. Tian, Y. S. Choi, B. I. Choi, S. Jon and W. K. Moon, *Theranostics*, 2014, **4**, 845–857.

60 Y. Du, X. Liu, Q. Liang, X.-J. Liang and J. Tian, *Nano Lett.*, 2019, **19**, 11.

61 M. Zuvin, M. Koçak, Ö. Ünal, Y. Akkoç and Ö. Kutlu, *J. Magn. Magn. Mater.*, 2019, **483**, 169–177.

62 B. Mol, A. Ereath, P. S. Jayaram, P. Prakash, R. S. Jayasree, S. Thomas, B. Chakrapani, M. R. Anantharaman and M. J. Bushiri, *J. Mater. Sci. Mater. Med.*, 2021, **32**, 108.

63 Y. Wei, R. Liao, A. Ahmed, H. Xu and Q. Zhou, *Acta Biomater.*, 2017, **55**, 194–203.

64 H. Vu-quang, M. S. Vinding, T. Nielsen and M. G. Ullisch, *Polymers*, 2019, **11**, 743.

65 M. Galli, B. Rossotti, P. Arosio, A. Maria, M. Panigati, E. Ranucci, P. Ferruti, A. Salvati and D. Maggioni, *Colloids Surf., B*, 2019, **174**, 260–269.

66 C. Martinelli, C. Pucci and G. Ciofani, *APL Bioeng.*, 2019, **3**, 011502.

67 Y. Wei, R. Liao, A. A. Mahmood, H. Xu and Q. Zhou, *Acta Biomater.*, 2017, **55**, 194–203.

68 H. Vu-Quang, M. S. Vinding, T. Nielsen, M. G. Ullisch, N. C. Nielsen, D. T. Nguyen and J. Kjems, *Polymers*, 2019, **11**, 743.

69 A. Patharkar, N. Raval, D. Kalyane, V. Tambe, N. Anup, N. More, G. Kapusetti, K. Kalia and R. K. Tekade, *J. Drug Delivery Sci. Technol.*, 2021, **61**, 102295.

70 A. Panahifar, M. Mahmoudi and M. R. Doschak, *ACS Appl. Mater. Interfaces*, 2013, **5**, 5219–5226.

71 L. Beola, L. Asín, C. Roma-Rodrigues, Y. Fernandez-Afonso, R. M. Fratila, D. Serantes, S. Ruta, R. W. Chantrell, A. R. Fernandes, P. V. Baptista, J. M. de la Fuente, V. Grazu and L. Gutierrez, *ACS Appl. Mater. Interfaces*, 2020, **12**, 43474–43487.

72 S. Fulda and K. M. Debatin, *Oncogene*, 2006, **25**, 4798–4811.

73 J. L. Roti, *Int. J. Hyperthermia*, 2008, **24**, 3–15.

74 A. Marino, A. Camponovo, A. Degl'Innocenti, M. Bartolucci, C. Tapeinos, C. Martinelli, D. De Pasquale, F. Santoro, V. Mollo, S. Arai, M. Suzuki, Y. Harada, A. Petretto and G. Ciofani, *Nanoscale*, 2019, **11**, 21227–21248.

75 S. Matsuda, E. Nakajima, T. Nakanishi, A. Hitsuji, H. Zhang, A. Tanaka, H. Matsuda, T. Momma and T. Osaka, *Mater. Sci. Eng., C*, 2017, **81**, 90–96.

76 S. E. Minaei, S. Khoei, S. Khoee, F. Vafashoar and V. P. Mahabadi, *Mater. Sci. Eng., C*, 2019, **101**, 575–587.

77 A. Riedinger, P. Guardia, A. Curcio, M. A. Garcia, R. Cingolani, L. Manna and T. Pellegrino, *Nano Lett.*, 2013, **13**, 2399–2406.

78 P. L. Silva, O. A. Savchuk, J. Gallo, L. García-Hevia, M. Bañobre-López and J. B. Nieder, *Nanoscale*, 2020, **12**, 21647–21656.

79 S. Du, J. Li, C. Du, Z. Huang, G. Chen and W. Yan, *Oncotarget*, 2017, **8**, 9410–9424.

80 G. Huang, H. Chen, Y. Dong, X. Luo, H. Yu, Z. Moore, E. A. Bey, D. A. Boothman and J. Gao, *Theranostics*, 2013, **3**, 116–126.

81 S. Klein, A. Sommer, L. V. R. Distel, W. Neuhuber and C. Kryschi, *Biochem. Biophys. Res. Commun.*, 2012, **425**, 393–397.

82 M. Mesárošová, K. Kozics, A. Bábelová, E. Regendová, M. Pastorek, D. Vnuková, B. Buliaková, F. Rázga and A. Gábelová, *Toxicol. Lett.*, 2014, **226**, 303–313.

83 J. E. Leadsham, G. Sanders, S. Giannaki, E. L. Bastow, R. Hutton, W. R. Naeimi, M. Breitenbach and C. W. Gourlay, *Cell Metab.*, 2013, **18**, 279–286.

84 K. Bedard and K. H. Krause, *Physiol. Rev.*, 2007, **87**, 245–313.

85 N. Yang, W. Xiao, X. Song, W. Wang and X. Dong, *Nano-Micro Lett.*, 2020, **12**, 15.

86 A. Sola-Leyva, Y. Jabalera, M. A. Chico-Lozano, M. P. Carrasco-Jiménez, G. R. Iglesias and C. Jimenez-Lopez, *J. Mater. Chem. B*, 2020, **8**, 7667–7676.

87 R. Gupta and D. Sharma, *ACS Appl. Nano Mater.*, 2020, **3**, 2026–2037.

88 R. Gupta and D. Sharma, *Colloids Surf., B*, 2021, **205**, 111870.

89 J. A. Zazo, G. Pliego, S. Blasco, J. A. Casas and J. J. Rodriguez, *Ind. Eng. Chem. Res.*, 2011, **50**, 866–870.

90 E. Cazares-Cortes, S. Cabana, C. Boitard, E. Nehlig, N. Griffete, J. Fresnais, C. Wilhelm, A. Abou-Hassan and C. Ménager, *Adv. Drug Delivery Rev.*, 2019, **138**, 233–246.

91 P. Boya and G. Kroemer, *Oncogene*, 2008, **27**, 6434–6451.

92 T. Kallunki, O. D. Olsen and M. Jäättelä, *Oncogene*, 2013, **32**, 1995–2004.

93 M. de Castro, G. Bunt and F. Wouters, *Cell Death Discovery*, 2016, **2**, 1–8.

94 M. Domenech, I. Marrero-Berrios, M. Torres-Lugo and C. Rinaldi, *ACS Nano*, 2013, **7**, 5091–5101.

95 C. Sanchez, D. El Hajj Diab, V. Connord, P. Clerc, E. Meunier, B. Pipy, B. Payré, R. P. Tan, M. Gougeon, J. Carrey, V. Gigoux and D. Fourmy, *ACS Nano*, 2014, **8**, 1350–1363.

96 C. Pucci, D. De Pasquale, A. Marino, C. Martinelli, S. Lauciello and G. Ciofani, *ACS Appl. Mater. Interfaces*, 2020, **12**, 29037–29055.

97 K. Glunde, S. E. Guggino, M. Solaiyappan, A. P. Pathak, Y. Ichikawa and Z. M. Bhujwalla, *Neoplasia*, 2003, **5**, 533–545.

98 K. Ono, S. O. Kim and J. Han, *Mol. Cell. Biol.*, 2003, **23**, 665–676.

99 S. Jeon, B. C. Park, S. Lim, H. Y. Yoon, Y. S. Jeon, B. S. Kim, Y. K. Kim and K. Kim, *ACS Appl. Mater. Interfaces*, 2020, **12**, 33483–33491.

100 M. Salimi, S. Sarkar, M. Hashemi and R. Saber, *Nanomaterials*, 2020, **10**, 1–18.

101 L. Beola, V. Grazú, Y. Fernández-Afonso, R. M. Fratila, M. De Las Heras, J. M. De La Fuente, L. Gutiérrez and L. Asín, *ACS Appl. Mater. Interfaces*, 2021, **13**, 12982–12996.

102 A. Chauhan, S. Midha, R. Kumar, R. Meena, P. Singh, S. K. Jha and B. K. Kuanr, *Biomater. Sci.*, 2021, **9**, 2972–2990.

103 D. A. Kedziorek, N. Muja, P. Walczak, J. Ruiz-Cabello, A. A. Gilad, C. C. Jie and J. W. M. Bulte, *Magn. Reson. Med.*, 2010, **63**, 1031–1043.

104 B. Sun, R. Liu, N. Ye and Z. D. Xiao, *PLoS One*, 2015, **10**, 1–11.

105 A. Albanese, P. S. Tang and W. C. W. Chan, *Annu. Rev. Biomed. Eng.*, 2012, **14**, 1–16.

106 G. Harris, T. Palosaari, Z. Magdolenova, M. Mennecozzi, J. M. Gineste, L. Saavedra, A. Milcamps, A. Huk, A. R. Collins, M. Dusinska and M. Whelan, *Nanotoxicology*, 2015, **9**, 87–94.

107 C. He, S. Jiang, H. Yao, L. Zhang, C. Yang, D. Zhan, G. Lin, Y. Zeng, Y. Xia, Z. Lin, G. Liu and Y. Lin, *Nanotoxicology*, 2018, **12**, 1198–1214.

108 E. Fröhlich, *J. Nanobiotechnol.*, 2017, **15**, 1–22.

109 A. L. Capriotti, C. Cavaliere and S. Piovesana, *Anal. Bioanal. Chem.*, 2019, **411**, 4313–4326.

110 C. Vogt, M. Pernemalm, P. Kohonen, S. Laurent, K. Hultenby, M. Vahter, J. Lehtiö, M. S. Toprak and B. Fadeel, *PLoS One*, 2015, **10**, 1–20.

111 D. Simberg, J. H. Park, P. P. Karmali, W. M. Zhang, S. Merkulov, K. McCrae, S. N. Bhatia, M. Sailor and E. Ruoslahti, *Biomaterials*, 2009, **30**, 3926–3933.

112 G. P. Smith, *Science*, 1985, **228**, 1315–1317.

113 G. P. Smith and J. K. Scott, *Methods in enzymology*, Elsevier, 1993, vol. 217, pp. 228–257.

114 A. C. W. Ch'ng, A. Ahmad, Z. Konthur and T. S. Lim, *Methods Mol. Biol.*, 2019, **1904**, 377–400.

115 S. Ghoshal, A. A. Ansar, S. O. Raja, A. Jana, N. R. Bandyopadhyay, A. K. Dasgupta and M. Ray, *Nanoscale Res. Lett.*, 2011, **6**, 1–8.

116 C. Carrara, PhD thesis, Università Degli Studi di Milano, 2012.

117 J. E. Blume, W. C. Manning, G. Troiano, D. Hornburg, M. Figa, L. Hesterberg, T. L. Platt, X. Zhao, R. A. Cuaresma and P. A. Everley, *Nat. Commun.*, 2020, **11**, 1–14.

118 A. K. Tharkeshwar, J. Trekker, W. Vermeire, J. Pauwels, R. Sannerud, D. A. Priestman, D. Te Vruchte, K. Vints, P. Baatsen and J.-P. Decuypere, *Sci. Rep.*, 2017, **7**, 1–20.

119 F. Akter, S. Ponnaiyan, B. Kögler-Mohrbacher, F. Bleibaum, M. Damme, B. Y. Renard and D. Winter, *bioRxiv*, 2020, DOI: 10.1101/2020.12.21.423747.

120 A. K. Tharkeshwar, D. Demedts and W. Annaert, *STAR Protoc.*, 2020, **1**, 100122.

121 P. Wust, U. Gneveckow, M. Johannsen, D. Böhmer, T. Henkel, F. Kahmann, J. Sehouli, R. Felix, J. Ricke and A. Jordan, *Int. J. Hyperthermia*, 2006, **22**, 673–685.

122 K. Maier-Hauff, R. Rothe, R. Scholz, U. Gneveckow, P. Wust, B. Thiesen, A. Feussner, A. Deimling, N. Waldoefner, R. Felix and A. Jordan, *J. Neurooncol.*, 2007, **81**, 53–60.

123 K. Maier-Hauff, F. Ulrich, D. Nestler, H. Niehoff, P. Wust, B. Thiesen, H. Orawa, V. Budach and A. Jordan, *J. Neurooncol.*, 2011, **103**, 317–324.

124 M. Johannsen, U. Gneveckow, B. Thiesen, K. Taymoorian, C. H. Cho, N. Waldöfner, R. Scholz, A. Jordan, S. A. Loening and P. Wust, *Eur. Urol.*, 2007, **52**, 1653–1662.

125 Magnetic Nanoparticle Thermoablation-Retention and Maintenance in the Prostate: A Phase 0 Study in Men – Full Text View – ClinicalTrials.gov, https://clinicaltrials.gov/ct2/show/NCT02033447, (accessed 25 November 2021).

126 A Phase I Clinical Trial of Neoadjuvant Chemotherapy With/Without SPIONs/SMF for Patients With Osteosarcoma – Full Text View – ClinicalTrials.gov, https://clinicaltrials.gov/ct2/show/study/NCT04316091, (accessed 25 November 2021).

127 M. Bassetto, D. Ajoy, F. Poulhes, C. Obringer, A. Walter, N. Messadeq, A. Sadeghi, J. Puranen, M. Ruponen, M. Kettunen, E. Toropainen, A. Urtti, H. Dollfus, O. Zelphati and V. Marion, *Pharmaceutics*, 2021, **13**, 1–21.

128 M. Szczęch, D. Orsi, N. Łopuszyńska, L. Cristofolini, K. Jasiński, W. P. Węglarz, F. Albertini, S. Kereïche and K. Szczepanowicz, *RSC Adv.*, 2020, **10**, 43607–43618.

129 H. Tran, N. M. Ngo, R. Medhi, P. Srinoi, T. Liu, S. Rittikulsittichai and T. R. Lee, *Materials*, 2022, **15**, 503.

130 D. Chang, M. Lim, J. A. C. M. Goos, R. Qiao and Y. Y. Ng, *Front. Pharmacol.*, 2018, **9**, 831.

131 Y. Gu, M. Yoshikiyo, A. Namai, D. Bonvin, A. Martinez, R. Piñol, P. Téllez, N. J. O. Silva, F. Ahrentorp, C. Johansson, J. Marco-Brualla, R. Moreno-Loshuertos, P. Fernández-Silva, Y. Cui, S. Ohkoshi and A. Millán, *RSC Adv.*, 2020, **10**, 28786–28797.

132 B. Chen, G. Chiu, Y. He, C. Huang, H. Huang, S. Sung, C. Hsieh, W. Chang, M. Hsu, Z. Wei and D. Yao, *PLoS One*, 2021, **16**, 1–19.

133 H. Wang, J. Wu, X. Zhang, Y. Liu, X. Zheng, Z. Zhuo and J. Tang, *J. Med. Biol. Eng.*, 2016, **36**, 726–732.

134 H. Wang, J. Wang, X. Wang, B. Zhang, Z. Xue, C. Qiu and J. Tang, 2020 IEEE 5th Int. Conf. Signal Image Process (ICSIP), pp. 1045–1049.